cmgh
CELLULAR AND MOLECULAR GASTROENTEROLOGY AND HEPATOLOGY

ORIGINAL RESEARCH

Hyperglycemia Enhances Immunosuppression and Aerobic Glycolysis of Pancreatic Cancer Through Upregulating Bmi1-UPF1-HK2 Pathway

Shihong Wu,[1,2,*] Haoxiang Zhang,[1,2,*] Chenggang Gao,[1,2,*] Jiaoshun Chen,[1,2] Hehe Li,[1,2] Zibo Meng,[2,3] Jianwei Bai,[1,2] Qiang Shen,[4] Heshui Wu,[1,2] and Tao Yin[1,2]

[1]Department of Pancreatic Surgery, Union Hospital, Tongji Medical College, Huazhong University of Science and Technology, Wuhan, China; [2]Sino-German Laboratory of Personalized Medicine for Pancreatic Cancer, Union Hospital, Tongji Medical College, Huazhong University of Science and Technology, Wuhan, China; [3]Division of Molecular Oncology of Gastrointestinal Tumors, German Cancer Research Center, Heidelberg, Germany; and [4]Department of Interdisciplinary Oncology, Louisiana State University Health Sciences Center, New Orleans, Louisiana

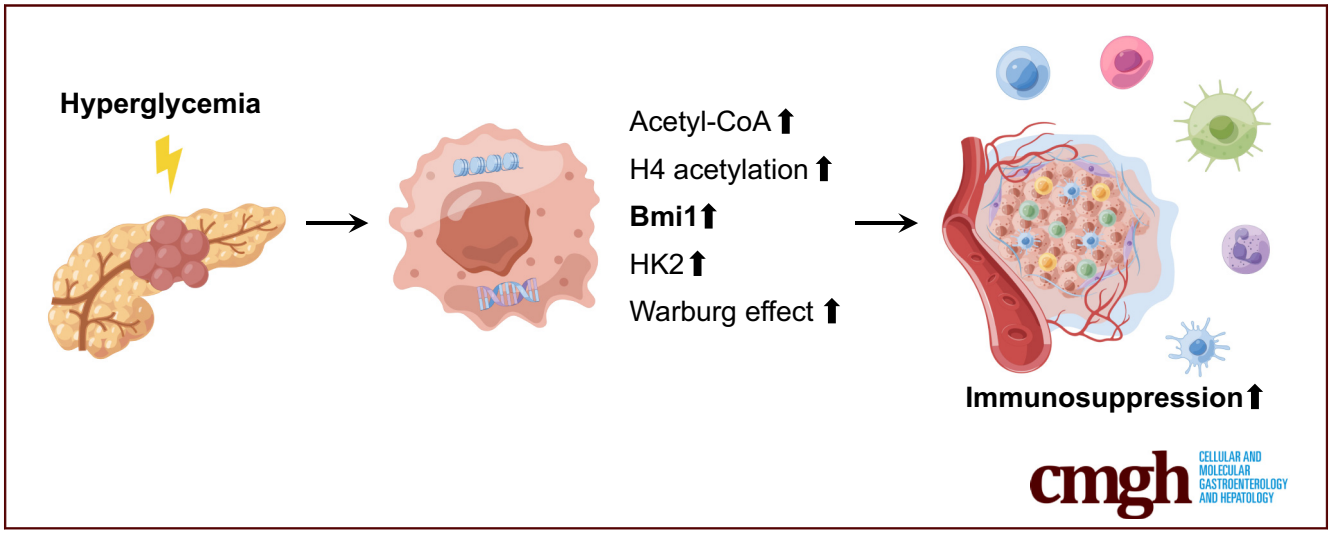

SUMMARY

Patients with pancreatic cancer complicated with diabetes mellitus have lower overall survival than those without. In this study, we define the role of Bmi1, a stemness-related oncogene, in controlling the Warburg effect, and immune suppression under hyperglycemia conditions through the unreported Bmi1-UPF1-HK2 pathway.

BACKGROUND & AIMS: Accumulating evidence strongly suggests that hyperglycemia promotes the progression of pancreatic cancer (PC). Approximately 80% of patients with PC are intolerant to hyperglycemic conditions. In this study, we define the role of Bmi1, a stemness-related oncogene, in controlling the Warburg effect, and immune suppression under hyperglycemia conditions.

METHODS: The diabetes mellitus model was established by intraperitoneal injection of streptozotocin. The role of the hyperglycemia-Bmi1-HK2 axis in glycolysis-related immunosuppression was examined in both orthotopic and xenograft in vivo models. Evaluation of immune infiltrates was carried out by flow cytometry. Human PC cell lines, SW1990, BxPC-3, and CFPAC-1, were used for mechanistic in vitro studies.

RESULTS: Through bioinformatics analysis, we found that hyperglycemia was strongly related to aerobic glycolysis, immunosuppression, and cancer cell stemness. High glucose condition in the tumor microenvironment promotes immune suppression by upregulating glycolysis in PC cells, which can be rescued via knockdown Bmi1 expression or after 2-deoxy-D-glucose treatment. Through gain-/loss-of-function assessments, we found that Bmi1 upregulated the expression of UPF1, which enhanced the stability of HK2 mRNA and thereby increased the expression of HK2. The role of the hyperglycemia-Bmi-HK2 pathway in the inhibition of antitumor immunity was further verified via the immune-competent and immunodeficient mice model. We also demonstrated that hyperglycemia promotes the expression of Bmi1 by elevating the intracellular acetyl-CoA levels and histone H4 acetylation levels.

CONCLUSIONS: Our results suggest that the previously unreported Bmi1-UPF1-HK2 pathway contributes to PC progression and immunosuppression, which may bring in new targets for developing effective therapies to treat patients with PC. *(Cell*

Mol Gastroenterol Hepatol 2022;14:1146–1165; https://doi.org/10.1016/j.jcmgh.2022.07.008)

Keywords: Aerobic Glycolysis; Bmi1; Hyperglycemic; Immunosuppression; Tumor Immune Microenvironment; Tumor Stemness.

Pancreatic cancer (PC) is one of the most lethal solid malignancies worldwide. Most patients with PC are in the advanced stage at the time of diagnosis, rendering a short window for very few available treatments.[1,2] It has been documented that diabetes mellitus (DM) is closely associated with PC, as DM is a risk factor for pancreatic carcinogenesis and progression.[3-7] Patients with PC complicated with DM have lower overall survival than those without.[8-11] A favorable management of blood glucose level improves the survival of PC patients, suggesting that hyperglycemia contributes to the progression of PC.[12,13]

Cancer cells prefer lactic acid fermentation to mitochondrial oxidative phosphorylation even in the presence of adequate oxygen, and can consume glucose at an exponential rate,[14] the phenomenon referred as to Warburg effect or "aerobic glycolysis." High glucose condition in the tumor microenvironment (TME) promotes glucose uptake and glycolytic activity in cancer cells.[15,16] Under aberrant glycolysis, lactic acid is accumulated in cells and then is exported into the extracellular environment, ultimately leading to the establishment of an acidic TME. Recent emerging evidence show that aerobic glycolysis not only plays a crucial role in promoting tumorigenesis and cancer progression but also impacts the anti-tumor immune response through multiple mechanisms.[17-19] Immune effector cells, including T cells and natural killer (NK) cells, tend to malfunction and undergo apoptosis when they are exposed to a low pH TME.[20-22] Aerobic glycolysis and immune evasion in cancer might be fundamentally related.[23,24] However, the molecular links between hyperglycemia and immune evasion of PC remains obscure.

Bmi1 is a major component of the polycomb group complex 1 (PRC1) and an oncogenic protein promoting the development of acute myeloid leukemia, breast cancer, nasopharyngeal carcinoma, and PC.[25-29] Bmi1 is also involved in regulating stemness, embryogenesis, and cancer drug resistance.[30-33] Intriguingly, Bmi1 is upregulated in PC cells under high glucose condition, contributing to immune suppression of NK cells.[34] However, whether Bmi1 is involved in metabolic reprogramming of PC and immune suppression of TME is poorly understood.

In this work, we investigated a previously unreported function of Bmi1 in PC cells that enhances aerobic glycolysis. Our results reveal a molecular mechanism in which hyperglycemia remodels the tumor-immune microenvironment via promoting Bmi1 expression through an epigenetic regulation. Our study thus brings in insights and new targets for intervening the malignant behavior of PC in the context of hyperglycemia.

Results

Hyperglycemia Promotes Immunosuppression in Patients With PC by Enhancing Aerobic Glycolysis

Glucose is the most important energy source molecule for cancer cells, and abnormal blood glucose level may significantly affect the metabolic propgram/reprogram of cancer cells. To investigate the association of hyperglycemia, aerobic glycolysis, and immunosuppression, we assessed the intensity of multiple metabolism pathways and infiltration of immune subsets in samples from a cohort (Array Expression /E-MTAB-6134), in which 309 samples were collected from consecutive patients who underwent surgery from September 1996 through December 2010 at 4 academic hospitals in Europe. In patients with PC, the level of glycolysis was negatively correlated with infiltration of $CD8^+$ T cells and dendritic cells (DCs), suggesting an immunosuppressive status (Figure 1, *A*). Compared with the low-glycolysis cohorts, high-glycolysis cohorts had poorer $CD8^+$ T cell infiltration ($P < .001$), DC infiltration ($P < .001$), and B cell infiltration ($P < .001$) (Figure 1, *B*). In addition, patients in the low-glycolysis cohorts had a better prognosis than those in the high-glycolysis cohorts ($P < .001$) (Array Expression /E-MTAB-6134) (Figure 1, *C*).

In vitro, the interferon-gamma (IFNγ)-positive cytotoxic T lymphocyte population was significantly lower in the high-glucose cohorts than those in the normal-glucose cohorts (Figure 2, *A*). Jurkat T cells cultured with differential glucose media for 48 hours showed dose-dependent increases of secreted interleukin (IL)-2 levels (Figure 2, *B*). This increase was blocked in co-culture with PC cells, and high glucose condition suppressed the Jurkat T cell's secretion of IL-2 compared with normal control cells (Figure 2, *C*). Each cell line showed that addition of glucose dose-dependently increased glucose uptake and lactate production (Figure 2, *D*), indicating upregulated glycolysis. Real-time quantitative polymerase chain reaction (RT-qPCR) analysis of mRNA showed upregulated SLC2A1, HK2, PKM2, and LDHA following high glucose treatment in PC cells cultured 48 hours under differential glucose concentrations (Figure 2, *E*). Western blot confirmed the protein levels matching the mRNA results (Figure 2, *F*). We then further investigated whether hyperglycemia promoted

***Authors share co-first authorship.**

Abbreviations used in this paper: **ACLY, ATP-citrate lyase; ChIP, chromatin immunoprecipitation assay; CSC, cancer stem cell; DC, dendritic cell; 2-DG, 2-deoxy-D-glucose; DM, diabetes mellitus; DMEM, Dulbecco's Modified Eagle Medium; H3ac, acetylation of histones H3; H4ac, acetylation of histones H4; IFNγ, interferon gamma; IHC, immunohistochemical; IL, interleukin; MAC, total macrophages; MDSCs, myeloid-derived suppressor cells; NC, nonsilencing; NK, natural killer; PBS, phosphate-buffered saline; PC, pancreatic cancer; PRC1, polycomb group complex 1; RT-qPCR, real-time quantitative polymerase chain reaction; shRNA, short hairpin RNA; siRNA, small interfering RNA; STZ, streptozocin; TME, tumor microenvironment; VPA, valproic acid.**

Most current article

2352-345X
https://doi.org/10.1016/j.jcmgh.2022.07.008

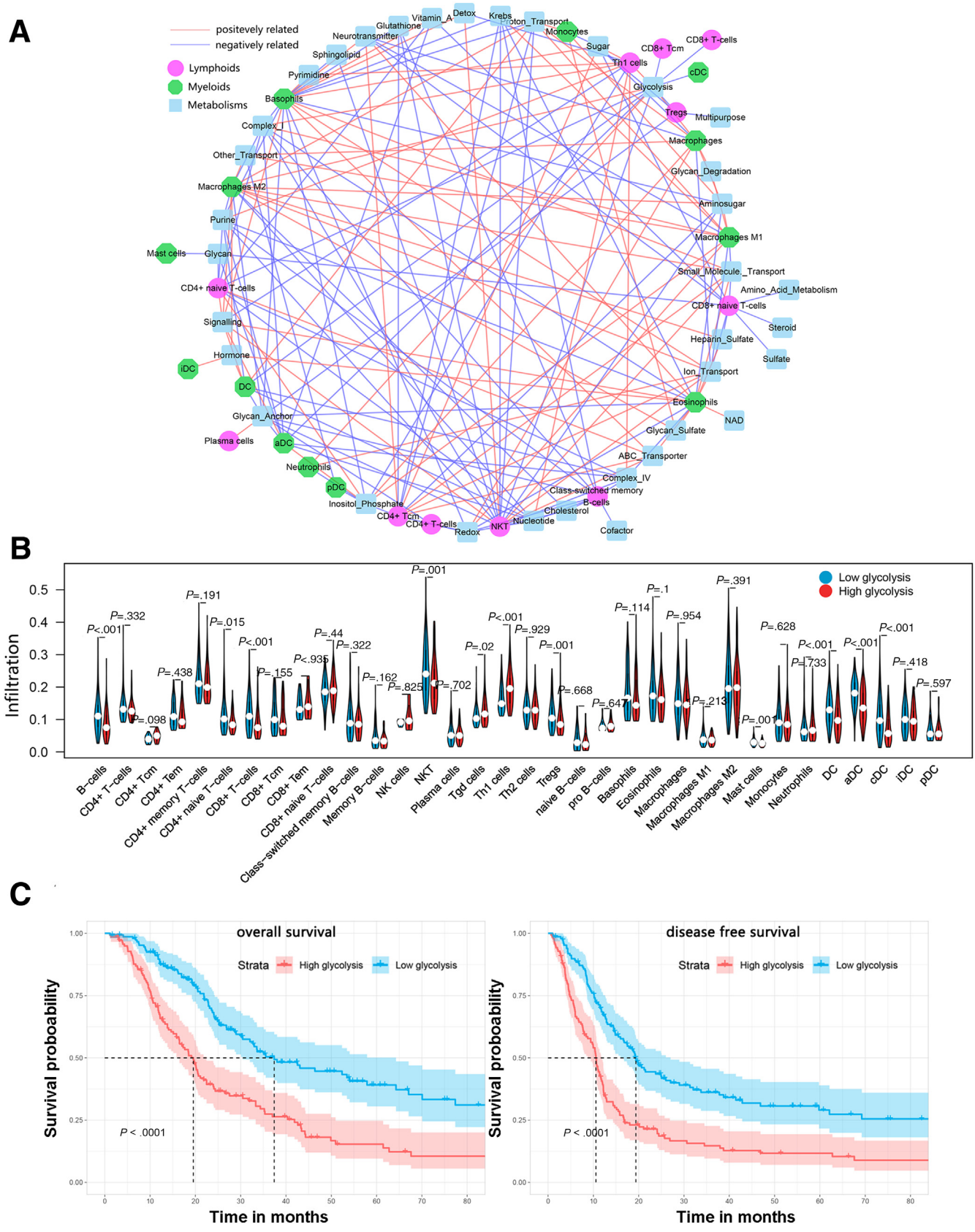

Figure 1. Association of aerobic glycolysis with PC immune evasion, survival, and cancer stemness. (*A*) Network plot depicting the relationship between multiple metabolisms and infiltrating immune subsets. (*B*) Violin plot depicting the status of infiltrating immune cells of samples with high or low glycolysis. (*C*) Survival analysis of patients with differential glycolytic statuses.

immune evasion via upregulating aerobic glycolysis in PC cells by determining whether inhibition of aerobic glycolysis rescues the activity of T lymphocytes and the infiltration of T-cells in xenografts. The SW1900 cells were pretreated with or without 2-deoxy-D-glucose (2-DG), a glycolysis inhibitor, for 24 hours and were then

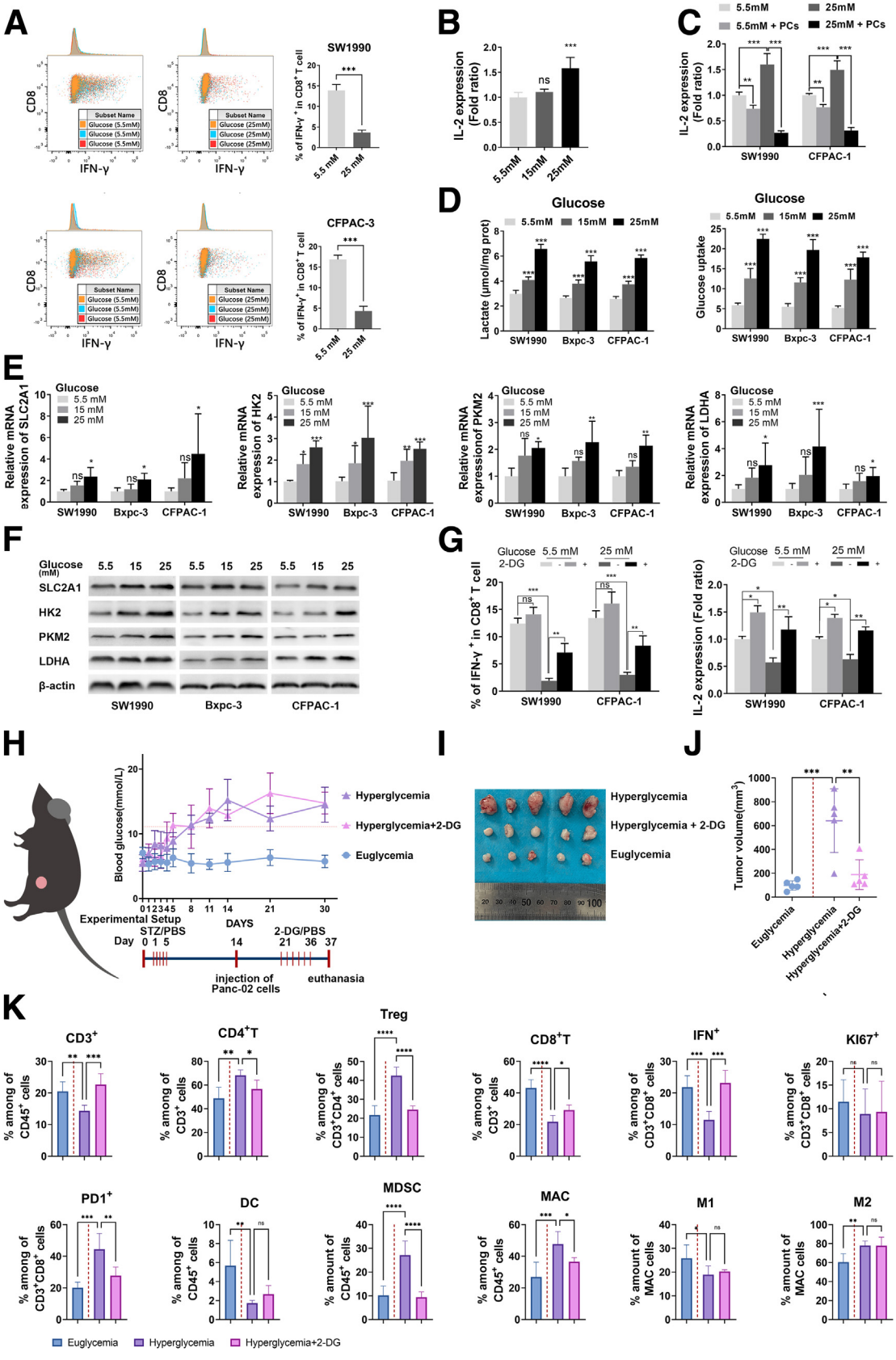

co-cultured with primary human T cells or Jurkat T-cells under differential glycemic conditions. As shown in Figure 2, *G*, 2-DG administration significantly rescued the immune effectors from the inhibitory effect of high glucose condition.

The in vitro results and the bioinformatic analysis result were further corroborated by in vivo assessments. A hyperglycemic mouse model was generated using streptozocin (STZ) to explore the role of hyperglycemia in immunosuppression in PC. The hyperglycemic mice had higher blood glucose levels than those in the control group (Figure 2, *H*). Compared with the euglycemic mice, tumors in hyperglycemic mice had greater tumor growth (Figure 2, *I–J*). Flow cytometry analysis showed sparser infiltration of immune effector cells, including $CD3^+CD8^+$ T cells, M1 macrophages, and DC cells in the xenografts. Subsequent immunophenotyping of mice showed that the $CD3^+CD8^+$ T cells were in an immunosuppressive state, exhibiting increased IFNγ and PD1 expression. The proportion of immunosuppressive cells, including Treg cells, total macrophages (MACs), M2 macrophages, and myeloid-derived suppressor cells (MDSCs) was dramatically higher in hyperglycemic mice (Figure 2, *K*).

Treatment with 2-DG or phosphate-buffered saline (PBS) was initiated 7 days after injecting Panc-02 cells in the right flank of hyperglycemic mice. The 2-DG treatment reduced subcutaneous tumor growth and reduced tumor weight in hyperglycemic mice compared with PBS-treated control mice (Figure 2, *I–J*). As shown in Figure 2, *K*, 2-DG administration partially rescued the immune effectors from hyperglycemic inhibition. Infiltrated immune cells in the subcutaneous tumors, including total $CD3^+$ T cells, $CD3^+CD8^+$ T cells, IFN-γ^+ of $CD8^+$ T, and DC cells, were higher in the 2-DG-treated hyperglycemic mice than in the PBS-treated control mice. The proportion of immunosuppressive cells such as $CD4^+$ Treg cells and MDSC was dramatically decreased. The PD-1^+ of $CD8^+$ T was also decreased in the 2-DG-treated group.

Correlation of Cancer Stemness, Aerobic Glycolysis, and Immune Evasion in Patients With PC

To further explore potential mechanisms regulating glycolysis and immune escape of PC, we explored the correlations between different signaling pathways, glycolysis, and immune infiltration in PC tissue samples through bioinformatics analysis using a publicly available database Array Expression/E-MTAB-1791, which contains RNA expression profiles of 195 pancreatic ductal adenocarcinoma frozen tissue. Interestingly, we found strong cross-correlations among stem cell signaling, glycolysis, and immune infiltration in PC (Figure 3, *A*).

To clarify the complicated cross correlations, we conducted correlation analysis among genes involved in stemness, glycolysis, and abundance of infiltrating immune cells. We found that stemness genes were strongly and positively related to glycolytic genes and that the latter exhibited inverse relationship to specific immune subsets including all subtypes of $CD8^+$ T-cells, $CD4^+$ T-cells, DCs, and NK cells, except Th2 cells, immature DCs, and macrophages, representing pro-tumor immune cell subsets (Figure 3, *B*). These results suggest a potential relationship among cancer stemness, aerobic glycolysis, and immune evasion.

To explore the potential effect of hyperglycemia on cancer stemness properties of PC cells, Western blotting, flow cytometry, and sphere formation assays were performed. Hyperglycemia enhanced the expression of the pluripotent cell markers including Nanog and Sox2, as well as the stemness markers including Oct4 and Klf4. We also noted that hyperglycemia promoted the expression of the pancreatic cancer stem cell (CSC) surface markers including CD133 and CD24 (Figure 3, *C*). Sphere formation assay further supported the above results (Figure 3, *D*). These findings demonstrate that a high glucose TME could potentially help PC cells to obtain more cancer stem-like properties.

High Glucose Condition Upregulated Bmi1 and Bmi1 Contributed to the High Glucose-enhanced Aerobic Glycolysis in PC Cells

PRC1 is an epigenetic gene silencer involved in the maintenance of embryonic and adult stem cells and tumorigenesis.[35] Bmi1, a component of PRC1, is involved in maintaining the pluripotency of pancreatic CSCs and the

Figure 2. (***See previous page***). **Hyperglycemia promotes T-cell immunosuppression in mice bearing PC by enhancing aerobic glycolysis.** (*A*) Flow cytometriy analysis of activated cytotoxic T-cell ($CD8^+$ IFN γ^+) population in co-culture with primary T-cells and pancreatic cancer cells in high glucose (25 mM glucose) culture condition compared with normal (5.5 mM glucose) culture conditions. (*B*) Bar graphs depicting levels of soluble IL-2 of Jurkat T-cells cultured in media with differential glucose concentrations. (*C*) Bar graphs depicting levels of soluble IL-2 of Jurkat T-cells in high glucose or normal conditions with or without the conditional media of PC cells. (*D*) Lactate production and uptake of 2-DG were measured in the medium of PC cells treated with differential concentrations of glucose for 48 hours. (*E*) qPCR analysis for SLC2A1, HK2, PKM2, and LDHA in PC cells treated with different concentrations of glucose for 48 hours. (*F*) Western blot for SLC2A1, HK2, PKM2, and LDHA proteins in PC cells treated with differential concentrations of glucose for 48 hours. (*G*) Bar graphs depicting flow cytometry analysis of activated cytotoxic T-cell (INFγ^+ and $CD8^+$) population and levels of soluble IL-2 in co-culture with primary T-cells and PC cells pretreated with or without 2-DG (5 mM) in high glucose culture conditions (25 mM glucose) compared with normal culture conditions (5.5 mM glucose). (*H*) Experimental schema of generating hyperglycemic mouse model and alterations in mouse blood glucose levels after STZ treatment. (*I*) Representative pictures of the subcutaneous tumors for immune-competent C57BL/6 mice in the euglycemic group, hyperglycemic group, and hyperglycemic 2-DG-treated group. (*J*) Changes in tumor volume of different groups. (*K*) Flow cytometry analysis of infiltrating immune effectors in the subcutaneous tumors of euglycemic group, hyperglycemic group, and hyperglycemic 2-DG-treated group. Data presented in the graphs represented means ± standard deviation from 3 parallel experiments. $^{****}P < .0001$; $^{***}P < .001$; $^{**}P < .01$; $^{*}P < .05$.

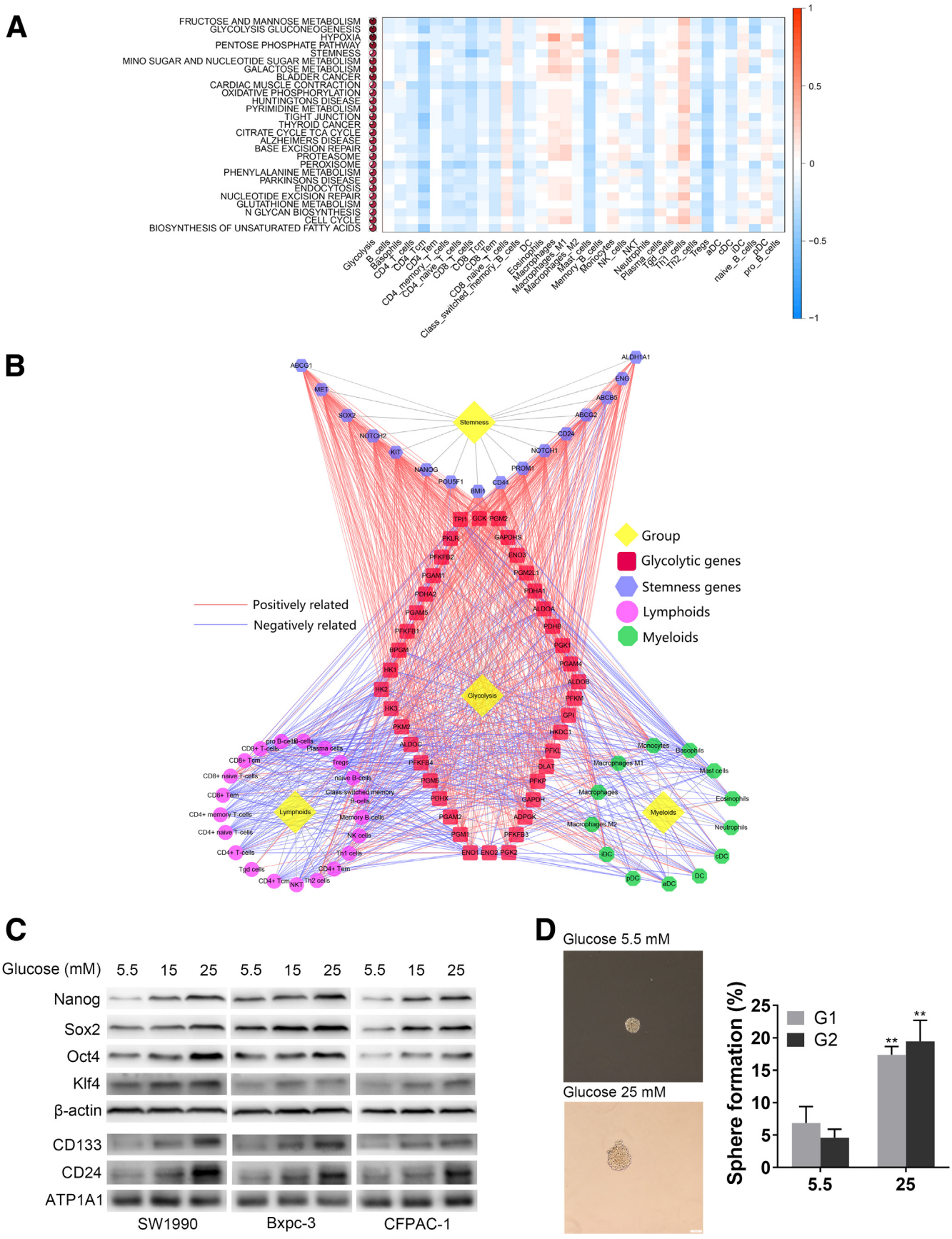
A
FRUCTOSE AND MANNOSE METABOLISM
GLYCOLYSIS GLUCONEOGENESIS
HYPOXIA
PENTOSE PHOSPHATE PATHWAY
STEMNESS
MINO SUGAR AND NUCLEOTIDE SUGAR METABOLISM
GALACTOSE METABOLISM
BLADDER CANCER
CARDIAC MUSCLE CONTRACTION
OXIDATIVE PHOSPHORYLATION
HUNTINGTONS DISEASE
PYRIMIDINE METABOLISM
TIGHT JUNCTION
THYROID CANCER
CITRATE CYCLE TCA CYCLE
ALZHEIMERS DISEASE
BASE EXCISION REPAIR
PROTEASOME
PEROXISOME
PHENYLALANINE METABOLISM
PARKINSONS DISEASE
ENDOCYTOSIS
NUCLEOTIDE EXCISION REPAIR
GLUTATHIONE METABOLISM
N GLYCAN BIOSYNTHESIS
CELL CYCLE
BIOSYNTHESIS OF UNSATURATED FATTY ACIDS
Glycolysis
B_cells
Basophils
CD4_Tcm
CD4_Tem
CD4_memory_T_cells
CD4_naive_T_cells
CD8_Tcm
CD8_Tem
CD8_naive_T_cells
Class_switched_memory_B_cells
DC
Eosinophils
Macrophages_M1
Macrophages_M2
Mast_cells
Memory B cells
Monocytes
NK_cells
NKT
Neutrophils
Plasma_cells
Tgd_cells
Th1_cells
Th2_cells
Tregs
aDC
cDC
naive_B_cells
pDC
pro_B_cells
1
0.5
0
−0.5
−1
B
Stemness
Glycolysis
Lymphoids
Myeloids
Positively related
Negatively related
Group
Glycolytic genes
Stemness genes
Lymphoids
Myeloids
C
Glucose (mM) 5.5 15 25 5.5 15 25 5.5 15 25
Nanog
Sox2
Oct4
Klf4
β-actin
CD133
CD24
ATP1A1
SW1990
Bxpc-3
CFPAC-1
D
Glucose 5.5 mM
Glucose 25 mM
Sphere formation (%)
G1
G2
5.5
25

initiation of PC.[29] It is highly expressed in human PC tissues as compared with normal pancreatic tissues[36,37] (Figure 4, *A*), which is associated with poor prognosis in PC.[28] Consistent with previous results,[34] high glucose condition dose-dependently increased Bmi1 mRNA and protein levels (Figure 4, *B*–*C*).

Metabolic reprogramming and cancer stemness are 2 closely related hallmarks of cancer.[38] CSCs have a relatively flexible metabolism, allowing them to adjust to variable TMEs.[39,40] Whether Bmi1 mediates high glucose enhancement of aerobic glycolysis in PC cells was determined by measuring lactate production and glucose uptake in PC cells overexpressing Bmi1 in high-glucose conditions. As shown in Figure 4, *D*–*F*, Bmi1 over-expression increased lactate production and glucose uptake in PC cells. Measuring glucose uptake and lactate production during Bmi1 silencing in PC cells cultured in differential glucose media showed that, in high-glucose conditions, Bmi1 silencing suppressed the upregulation of aerobic glycolysis (Figure 4, *G*–*I*).

Bmi1 Promotes Aerobic Glycolysis in PC Cells via UPF1-HK2 Signaling Pathway

We further explored the mechanism underlying Bmi1, the stem cell factor, promoting glycolysis in PC. Protein expression of SLC2A1, HK2, PKM2, and LDHA was measured after Bmi1 upregulation in PC cells. Ectopic expression of Bmi1 increased protein levels of HK2, whereas SLC2A1, PKM2, and LDHA did not respond to Bmi1 overexpression (Figure 5, *A*). Knocked-down Bmi1 expression dramatically blocked HK2 upregulation under high-glucose treatment in all 3 PC cell lines (Figure 5, *B*).

To explore Bmi1 induction of HK2 expression, we searched the GEPIA2 website (http://gepia2.cancer-pku.cn/#index) for genes co-expressed with Bmi1 and HK2 in PC. UPF1, an RNA-binding protein, was found to closely correlate with Bmi1 and HK2 in PC (Figure 5, *C*–*F*). Transient expression of Bmi1 in PC cells promoted UPF1 protein expression as compared with cells with vector control (Figure 5, *E*). UPF1 silencing suppressed the Bmi1-induced upregulation of HK2 expression (Figure 5, *F*). Because UPF1 is an RNA-binding protein, whether UPF1 promotes HK2 expression by stabilizing its mRNA was determined. An RNA immunoprecipitation experiment showed that the relative enrichment level of HK2 mRNA was higher in the anti-UPF1 samples than that in the anti-normal group (Figure 5, *G*), indicating that UPF1 promoted the stability of HK2 mRNA. To confirm this finding, the half-life of HK2 mRNA was measured after knocking-down of UPF1. The half-life of HK2 mRNA in the UPF1-silenced group was decreased (Figure 5, *H*). These results suggest that high-glucose-induced Bmi1 upregulation promotes aerobic glycolysis by inducing HK2 in an UPF1-dependent manner.

To test whether Bmi1 promotes aerobic glycolysis through HK2, PC cells were treated with 2-DG, which cannot be further metabolized via glycolysis but accumulates and non-competitively inhibits HK and competitively inhibits PGI, after overexpression of Bmi1. Treatment with 2-DG blocked the upregulated lactate production that was induced by Bmi1 overexpression (Figure 5, *I*). Taken together, these results demonstrate that the Bmi1-UPF1-HK2 signaling pathway plays a key role in regulating aerobic glycolysis in PC cells.

Bmi1-HK2 Pathway is Involved in Immunosuppression

Whether Bmi1-HK2 signaling pathway is involved in aerobic glycolysis-induced immunosuppression was first examined by co-culturing activated human primary T cells with PC cells in vitro. Flow cytometry analysis showed that 2-DG treatment reversed the inhibitory effects of Bmi1 on the activity of T cells (Figure 5, *J*–*K*).

We then verified this hypothesis in vivo. To exclude the direct effect of 2-DG on glycolysis on immune cells in the tumor microenvironment, we employed rescue experiments via direct knock-down or overexpression of HK2 with lentivirus infection approach and validated the impact of Bmi1-HK2 activation/downregulation on immunosuppression. Stable Panc-02 cells transfected with nonsilencing (NC), OE-Bmi1, KD-Bmi1, OE-Bmi1/KD-HK2, KD-Bmi1/OE-HK2, or KD-HK2 lentivirus were injected into the C57BL/6 mice pancreas tail by laparotomy (Figure 6, *A*–*B*). Under euglycemic conditions, OE-Bmi1 expression *in vivo* promoted the tumorigenesis and KD-HK2 expression partly rescued this effect. KD-HK2 expression or KD-Bmi1 expression in vivo suppressed the tumorigenesis induced by hyperglycemic conditions, and OE-HK2 rescued the potential therapeutic efficacy of KD-Bmi1 (Figure 6, *C*). T-cells, DC, MDSC and MAC were evaluated by flow cytometry analysis (Figure 6, *E*). Our results show that Bmi1-overexpressed tumors had less infiltrated $CD3^+$ T cells, $CD3^+CD8^+$ T cells, DC cells, and higher $CD8^+PD1^+$ T cells, and MDSC than controls. Moreover, this effect could be reversed by KD-HK2. Under hyperglycemic conditions, Bmi1 inhibition could recover the anti-tumor immune cell infiltration including $CD3^+CD8^+$ T cells. Enhanced $CD8^+$ T cells function (IFN-γ^+CD8^+ T cells and $GZMB^+CD8^+$ T cells) and reduced infiltration of $CD4^+$ Treg, PD-1^+CD8^+T cells, and MAC were also detected. Importantly, this effect can be

Figure 3. (***See previous page***). **High glucose condition promotes the stemness of PC cells.** (*A*) Heat map depicting the relationship among different signaling pathways, glycolysis, and immune infiltration in pancreatic tumors. (*B*) Network anaylis depicting the relationship among genes involved in stemness, glycolysis, and immune infiltration. (*C*) Western blot for Nanog, Sox2, Klf4, and Oct4 protein expression in PC cells and CD133 and CD24 expression on the cell surface in SW1990, Bxpc-3, and CFPAC-1cells treated with differential glucose treatment for 48 hours. (*D*) Sphere-forming ability of PC cells of generation 1 and generation 2 in the serum-free medium under high glucose or normal glucose conditions, scale bar, 100 μm. Data presented in the graphs represented means ± standard deviation from 3 parallel experiments. ***$P < .001$; **$P < .01$; *$P < .05$.

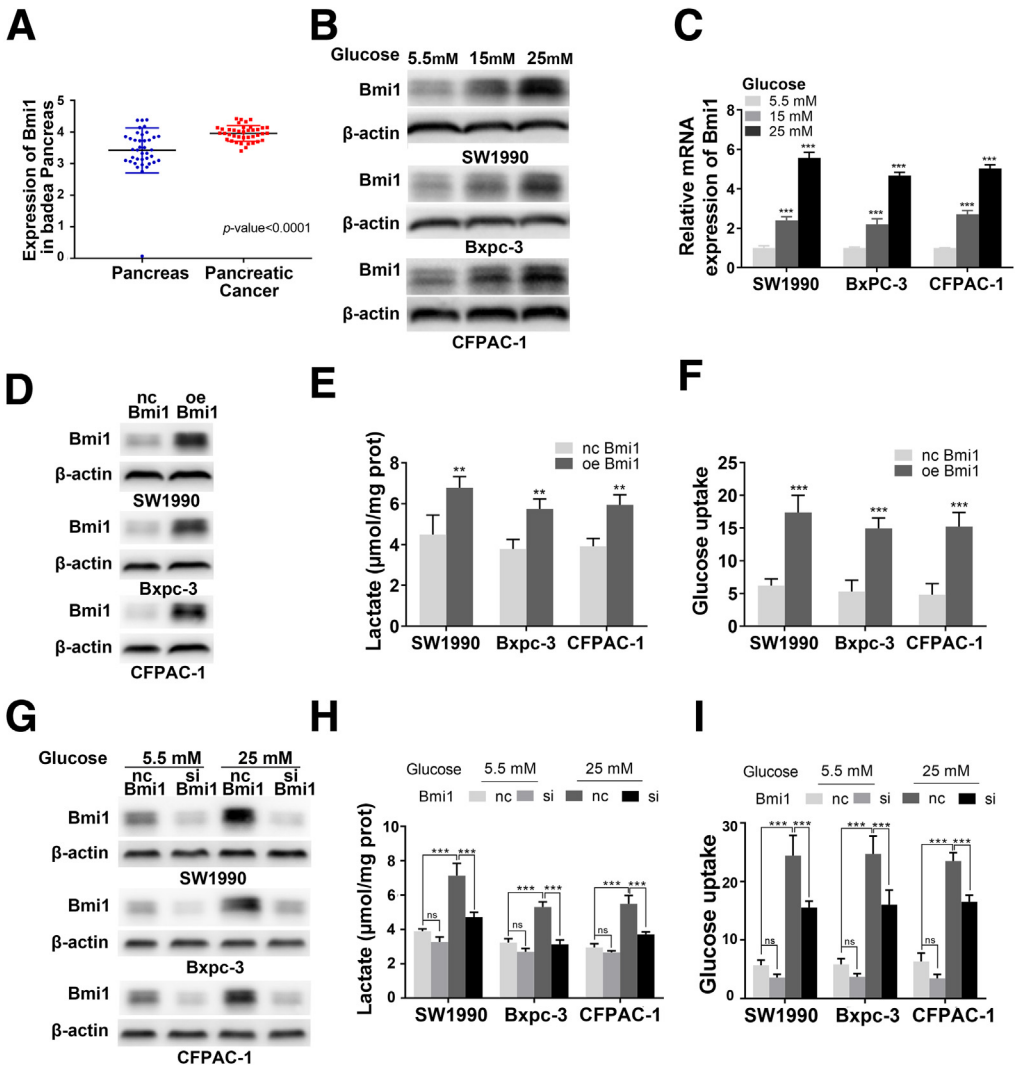

Figure 4. Bmi1 was upregulated in high glucose conditions and contributed to the high glucose-enhanced aerobic glycolysis in PC cells. (*A*) In silico analysis demonstrating Bmi1 mRNA expression level in normal pancreatic tissue samples (n = 39) and pancreatic ductal adenocarcinoma tissue samples (n = 39). (*B*) Western blot of Bmi1 protein in PC cells treated with differential concentrations of glucose for 48 hours. (*C*) Bmi1 mRNA expression in the cells in *A*. (*D*) Western blot of Bmi1 protein in PC cells transfected with vector or Bmi1 plasmid. (*E*) Lactate production was measured in the supernatant of PC cells transfected with vector or Bmi1 plasmid. (*F*) Uptake of glucose was measured by flow cytometry in PC cells transfected with vector or Bmi1 plasmid. (*G*) Western blot of Bmi1 protein in PC cells transfected with vector or Bmi1 plasmid under high glucose or normal conditions. (*H*) Lactate production was measured in the medium of PC cells after transfection with ncRNA or Bmi1 siRNA under high glucose or normal conditions. (*I*) Uptake of glucose was measured by flow cytometry in PC cells after transfection with ncRNA or Bmi1 siRNA under high glucose or normal conditions. Data presented in the graphs represented means ± standard deviation from 3 parallel experiments. ***$P < .001$; **$P < .01$; *$P < .05$.

reversed by OE-HK2. Taken together, our results demonstrate that Bmi1-HK2 activation inhibits the function of immune effectors in the TME of PC.

High Glucose Condition Induces Bmi1 Expression Through ATP-citrate Lyase-dependent Acetyl-CoA

We further explored the mechanism underlying Bmi1 induction under a high glucose environment. Because acetyl-CoA is the necessary donor substrate of histone lysine acetyltransferase (KAT) enzymes,[41] the intracellular acetyl-CoA levels of PC cells were determined in different glycemic conditions. High-glucose treatment dose-dependently increased intracellular acetyl-CoA levels. Western blot analysis of ATP-citrate lyase (ACLY), which synthesizes acetyl-CoA, showed that PC cells treated with high glucose had higher levels of ACLY than those treated with normal glucose (Figure 7, *A*).

To test whether hyperglycemic-induced Bmi1 upregulation was due to the accumulation of intracellular acetyl-CoA, we tested 3 ACLY-specific small interfering RNAs (siRNAs) in 3 PC cell lines (SW1990, Bxpc-3, and CFPAC-1) (Figure 7, *A*). The most significant knockdown effect was found with

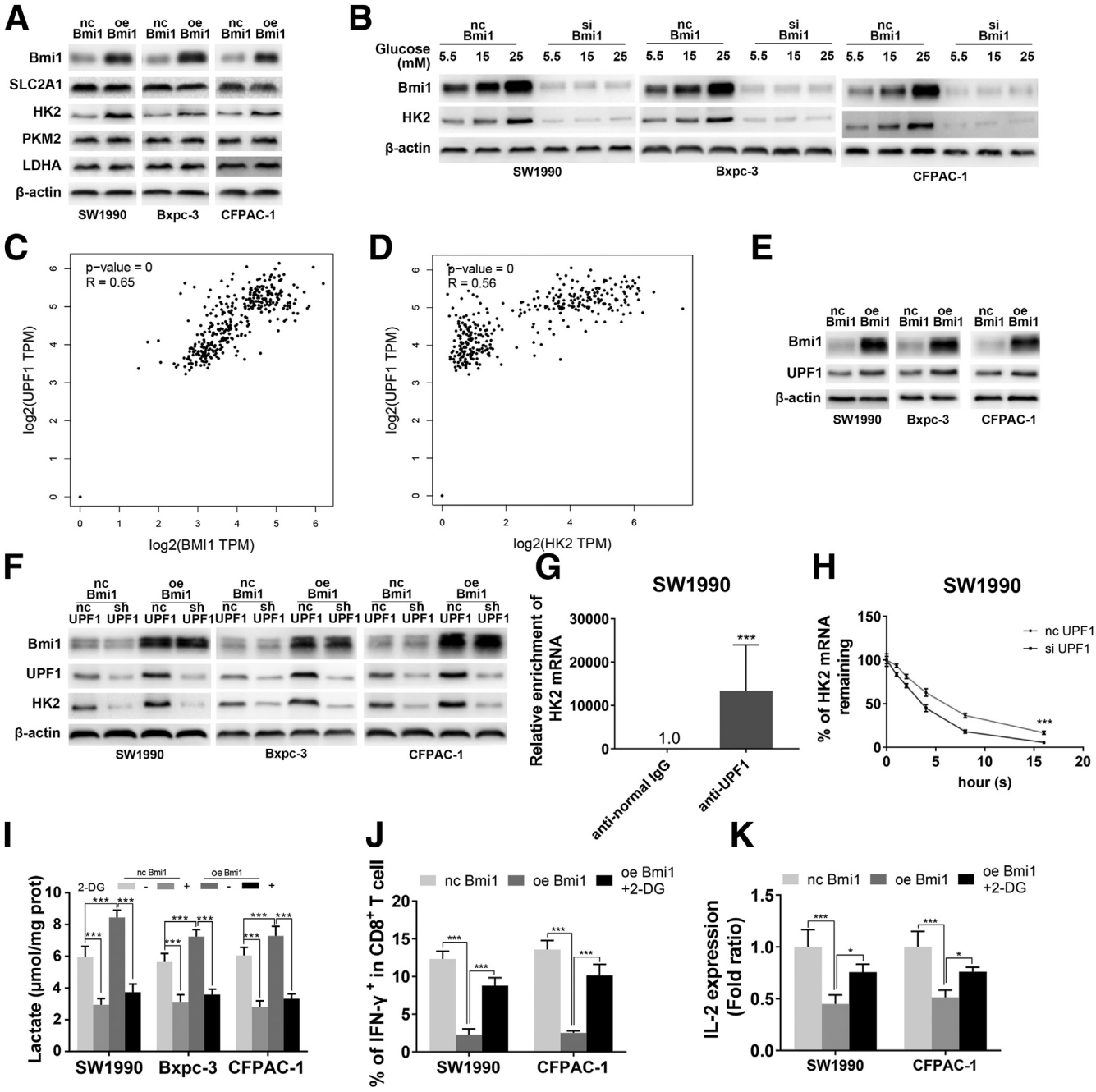

Figure 5. Bmi1-UPF1-HK2 pathway promotes aerobic glycolysis in PC cells. (*A*) Western blot of Bmi1, SLC2A1, HK2, PKM2, and LDHA protein in PC cells transfected with vector or Bmi1 plasmid. (*B*) Western blot of Bmi1 and HK2 protein in PC cells after transfection with ncRNA or Bmi1 siRNA under different glycemic conditions. (*C*) The GEPIA web tool was adopted to search for the correlation between the expression of Bmi1 and UPF1 in mRNA level in pancreatic ductal adenocarcinoma samples. *P* values as indicated in the Figure. (*D*) The GEPIA web tool was adopted to search for the correlation between the expression of UPF1 and HK2 at mRNA levelsin pancreatic ductal adenocarcinoma samples. *P*-values as indicated in the Figure. (*E*) Western blot of Bmi1 and UPF1 protein in PC cells transfected with vector or Bmi1 plasmid. (*F*) Western blot of Bmi1, UPF1, and HK2 protein in sh-control or sh-UPF1 PC cells transfected with vector or Bmi1 plasmid. (*G*) RNA immunoprecipitation (RIP) assay was used to detect the binding between UPF1 and HK2 mRNA. (*H*) HK2 mRNA half-life measured by qRT-PCR after actinomycin D treatment. (*I*) Bar graphs depicting lactate production with or without 2-DG (5 mM) in PC cells after transfection with ncRNA or Bmi1 oeRNA. Data presented in the graphs represented means ± standard deviation from 3 parallel experiments. (*J*) Bar graphs depicting flow cytometric analysis of activated cytotoxic T-cell ($INF\gamma^+$ and $CD8^+$) population in co-culture of primary T-cells and PC cells transfected with vector or Bmi1 plasmid pretreated with or without 2-DG (5 mM). (*K*) Bar graphs depicting the levels of soluble IL-2 of Jurkat T-cells with the conditional medium of PC cells transfected with vector or Bmi1 plasmid pretreated with or without 2-DG (5 mM). ***$P < .001$; **$P < .01$; *$P < .05$.

siACLY#003, which was employed in the following studies (Figure 7, *B*). ACLY knockdown prevented intracellular acetyl-CoA increase due to hyperglycemia in SW1990, Bxpc-3, and CFPAC-1 cells (Figure 7, *C*). High-glucose-induced Bmi1 overexpression was also inhibited by ACLY knockdown (Figure 7, *D*), suggesting that Bmi1 induction is acetyl-CoA-dependent. High-glucose treatment increased the acetylation of histones H3 (H3ac) and H4 (H4ac) (Figure 7, *E*); this effect was inhibited by the knockdown of ACLY (Figure 7, *F*).

Acetyl-CoA levels were increased by acetate supplementation to test how high glucose levels promote Bmi1 expression in PC cells. Levels of intracellular acetyl-CoA, H3ac, H4ac, and Bmi1 expression increased after acetate supplementation (Figure 7, *G*–*H*). Moreover, acetate supplementation reversed the suppression of H3ac, H4ac, and Bmi1 expression in PC cells caused by ACLY silencing (Figure 7, *I*). Therefore, increased intracellular acetyl-CoA is essential for high-glucose-induced Bmi1 expression in PC cells.

Bmi1 Expression is Enhanced by Upregulating Histone H4 Acetylation

Valproic acid (VPA), an inhibitor of histone deacetylase I, increases Bmi1 expression in PC cells[42] and was used to determine whether histone acetylation was involved in the high glucose–induced Bmi1 expression in PC cells. To test whether acetylation of histone H3 and H4 is required for enhanced Bmi1 expression, PC cells were treated with VPA or C646, a p300 acetyltransferase inhibitor. VPA promoted Bmi1 expression and upregulated H3ac and H4ac levels in PC cells (Figure 8, *A*). Furthermore, low-dose VPA reversed the inhibitory effect of ACLY silencing on H3 and H4 acetylation and Bmi1 expression in PC cells (Figure 8, *B*). C646 treatment of PC cells suppressed the H3 and H4 acetylation and Bmi1 expression induced by high-glucose treatment (Figure 8, *C*) and reversed the increase of H3 and H4 acetylation and Bmi1 expression caused by acetate supplementation (Figure 8, *D*).

Because high glucose, ACLY knockdown, acetate supplementation, VPA, and C646 affected both H3ac and H4ac, the KATs that are responsible for H3/H4 acetylation were knocked down. Knockdown of KAT5, which acetylates H4, inhibited high-glucose-induction of Bmi1 expression, but KAT2A, which acetylates H3, did not (Figure 8, *E*–*F*). To confirm this, chromatin immunoprecipitation assays (ChIPs) were conducted using SW1990 cells cultured in normal or high-glucose media. Measurement of H3ac and H4ac levels in the Bmi1 gene promoter region showed that H4ac levels were higher in cells treated with high glucose than in those treated with normal glucose (Figure 8, *G*). These results suggest that a high-glucose environment promotes Bmi1 expression in PC cells through upregulating H4 acetylation levels in the promoter region of the Bmi1 gene.

The Role of Hyperglycemia-induced Bmi1 Under Immunodeficient Environment

To verify the in vitro findings and evaluate the role of hyperglycemia and Bmi1 in tumorigenesis under an immunodeficient environment, subcutaneous Panc-02 model in immunodeficient BALB/c nude mice was built with stable Panc-02 cells infected by NC, OE-Bmi1, and KD-Bmi1 lentivirus in both euglycemia and hyperglycemic mice (Figure 9, *A*). Compared with the euglycemic mice, the tumors in hyperglycemic mice had greater tumor growth (Figure 9, *B*).

As shown in Figure 9, *D*, hyperglycemia increased the content of glucose and lactate in subcutaneous tumor tissues. As determined using an immunohistochemical (IHC) assessment, hyperglycemia increased the expression level of ACLY, KAT5, H4ac, and Bmi1 (Figure 9, *E*). Bmi1 has been well-known for its abilities in controlling stem cell self-renewal and tissue homeostasis. Therefore, both in OE-Bmi1 under euglycemia model or KD-Bmi1 under hyper-euglycemia model, Bmi1 contributed some degree of proliferation of tumor cells in immunodeficient mice model (Figure 9, *B*). However, we can find that KD-Bmi1 completely inhibited tumor outgrowth promoted by hyperglycemia in immunocompetent mice (Figure 5, *C*–*D*). Although in immunodeficient mice, KD-Bmi1 only partially inhibit tumor outgrowth promoted by hyperglycemia (Figure 9, *B*–*C*). We believe that this difference in rescue experiments was caused by Bmi1-mediated immunosuppression, as supported by our data. The expression of UPF1 and HK2 was regulated by Bmi-1 in vivo (Figure 9, *F*). Next, we validated UPF1 and HK2 expression in KD-Bmi1, NC, and OE-Bmi1 cells by performing IHC staining (Figure 9, *F*).

Discussion

Hyperglycemia is associated with most patients with PC, suggesting a role of glucose level in PC progression, immune suppression, and therapeutic outcomes. This study focused on the interactions between hyperglycemia and PC carcinogenesis, leading to the discovery of a previously unreported Bmi1-UPF1-HK2 signaling pathway in pancreatic carcinogenesis. This pathway regulates aerobic glycolysis, leading to enhanced Warburg effect and the establishment of an immunosuppressive TME, by upregulating intracellular acetyl-CoA and histone H4 acetylation to upregulate Bmi1 expression (Figure 7, *G*). Results presented in this paper provide evidence that a high glucose condition in pancreatic TME facilitates PC to evade immune surveillance via upregulating aerobic glycolysis in PC cells. These findings enhance our understanding of PC progression and immune suppression and provide insights for developing targeted cancer and immune therapies for this deadly malignancy.

The relationship between diabetes and PC is complicated. Hyperglycemia is characteristic of diabetes, a risk factor for PC, and associated with poor survival among PC patients.[9,11,43,44] Acumulating epidemiological data suggest that PC maybe an etiological factor of diabetes with unknown mechanisms.[45-47] On the other hand, factors such as insulin resistance, hyperinsulinemia, high levels of insulin-like growth factor 1, inflammation, and hyperglycemia are suggested to be potential underlying mechanisms contributing to the progression of PC, which is further complicated

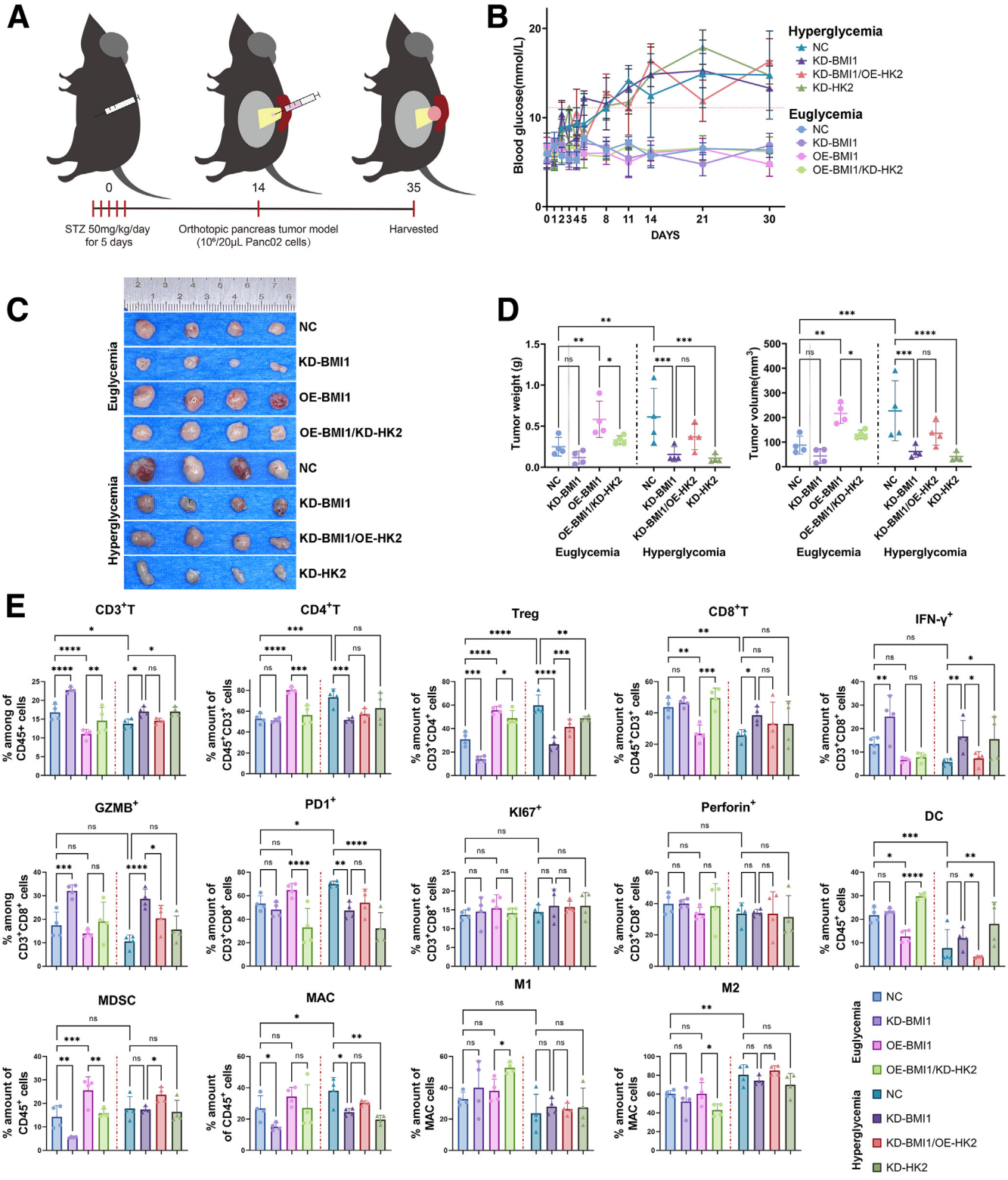

Figure 6. Bmi1-HK2 signaling is involved in T cell immunosuppression in PC. (*A*) Experimental schema of generating hyperglycemic mouse model. (*B*) Alterations in blood glucose levels after STZ treatment in mice. (*C*) Representative pictures of the orthotopic tumors. (*D*) Changes in tumor volume and tumor weight in animals. (*E*) Flow cytometry analysis of the infiltration of immune effectors ($CD3^+$T, $CD3^+CD4^+$ T, Treg, $CD3^+CD8^+$T, IFN-γ^+ $CD8^+$T, $GZMB^+$ $CD8^+$T, $PD1^+$ $CD8^+$T, $KI67^+$ $CD8^+$T, $Perforin^+$ $CD8^+$T, DC, MDSC, MAC, M1 macrophages, M2 macrophages) in the orthotopic tumors in different groups. Data presented in the graphs represented means ± standard deviation from 3 parallel experiments. $^{****}P < .0001$; $^{***}P < .001$; $^{**}P < .01$; $^{*}P < .05$.

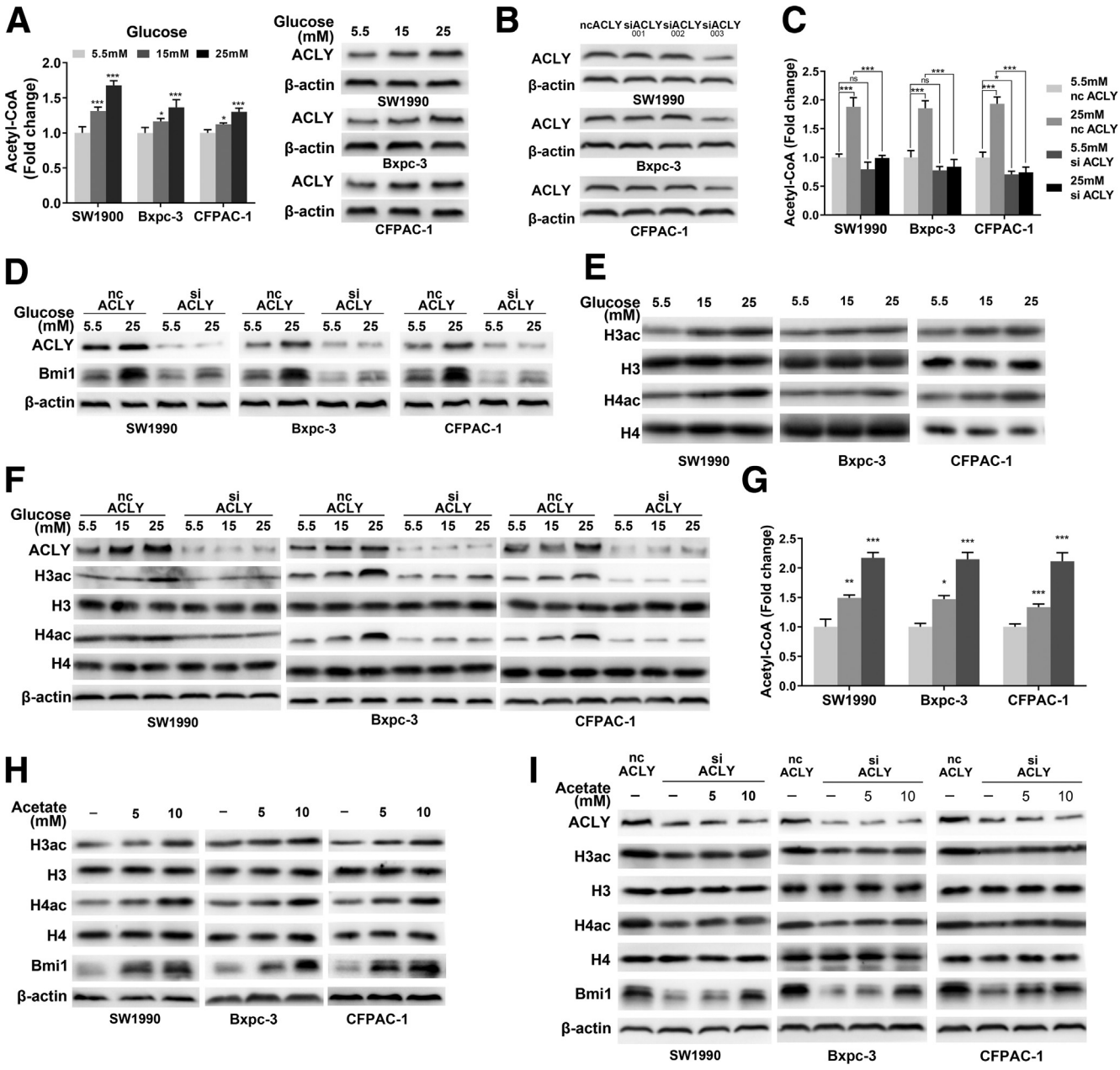

Figure 7. Acetyl-CoA is required for Bmi1 induction under high glucose condition in PC cells. (*A*) Bar graphs depicting levels of intracellular acetyl-CoA and Western blot of ACLY protein in PC cells under different glycemic conditions. (*B*) Western blot of ACLY and Bmi1 proteins in PC cells transfected with ncRNA or ACLY siRNA. (*C*) Bar graphs depicting levels of intracellular acetyl-CoA in PC cells transfected with ncRNA or ACLY siRNA under high glucose or normal conditions. (*D*) Western blot of ACLY and Bmi1 proteins in PC cells transfected with ncRNA or ACLY siRNA under high glucose or normal conditions. (*E*) Western blot of histone H3ac and H4ac proteins in PC cells under different glycemic conditions. (*F*) Western blot of ACLY, histone H3ac, and H4ac proteins in PC cells transfected with ncRNA or ACLY siRNA under different glycemic conditions. (*G*) Bar graph depicting levels of intracellular acetyl-CoA in PC cells treated with acetate. (*H*) Western blot of histone H3ac, histone H4ac, and Bmi1 proteins in PC cells treated with acetate. (*I*) Western blot of ACLY, histone H3ac, histone H4ac, and Bmi1 proteins in ACLY knockdown PC cells treated with or without acetate. Data presented in the graphs represented means ± standard deviation from 3 parallel experiments. ***$P < .001$; **$P < .01$; *$P < .05$.

with diabetes.[43] High glucose condition promotes epithelial-mesenchymal transition and proliferation of PC cells,[48,49] and suppresses the cytotoxic effects of NK cells on PC cells via the AMPK-Bmi1-GATA2-MICA/B pathway, suggesting that high glucose may play an important role in the development of immunosuppressive milieu.[34] Although the mechanisms by which high glucose condition affects metabolic reprogramming have yet to be fully determined,

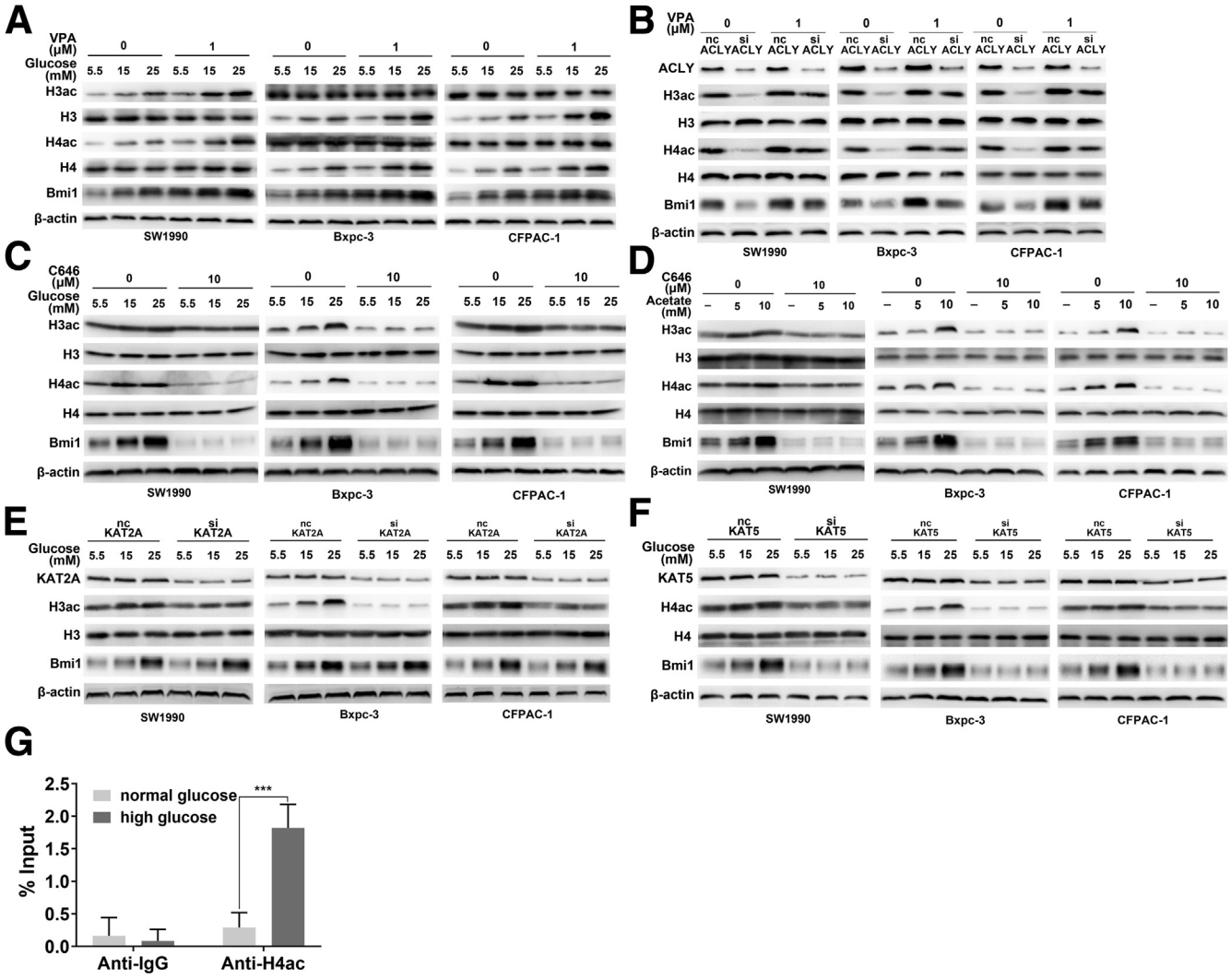

Figure 8. Histone acetylation is required for Bmi1 induction under high glucose condition in PC cells. (*A*) Western blot of histone H3ac, histone H4ac, and Bmi1 proteins in PC cells treated with or without VPA under different glycemic conditions. (*B*) Western blot of ACLY, histone H3ac, histone H4ac, and Bmi1 proteins in ACLY knockdown PC cells treated with or without VPA. (*C*) Western blot of histone H3ac, histone H4ac, and Bmi1 proteins in PC cells treated with or without C646 under different glycemic conditions. (*D*) Western blot of histone H3ac, histone H4ac, and Bmi1 proteins in PC cells treated with or without C646 under different concentrations of acetate. (*E*) Western blot of KAT2A, histone H3ac, and Bmi1 proteins in PC cells transfected with ncRNA or KAT2A siRNA under different glycemic conditions. (*F*) Western blotof KAT5, histone H4ac, and Bmi1 proteins in PC cells transfected with ncRNA or KAT5 siRNA under different glycemic conditions. (*G*) Examination of histone H4 acetylation status in the Bmi1 gene promoter region in PC cells under high glucose or normal conditions using ChIP.

this study suggests that hyperglycemia induces Bmi1 expression by binding of H4ac in the promoter of Bmi1 gene. This upregulates the Bmi1-UPF1-HK2 signaling pathway, which promotes aerobic glycolysis and lactate production in PC cells and leads to immune suppression. This suggests that Bmi1 is a novel potential therapeutic target for patients with PC complicated with diabetes.

Glucose is an important energy source for cancer cells. When immersed in an environment with excessive nutrients, cancer cells tend to upregulate their nutrient uptake and adopt aerobic glycolysis to generate intermediate metabolites,[50,51] suggesting that PC cells cultured in a high glucose medium may upregulate aerobic glycolysis activity. This hypothesis was confirmed by the results in this study. Because CSCs have metabolic plasticity in response to variable TMEs,[39,40] the stemness-related gene Bmi1[29,31] was suggested to be involved in hyperglycemia-induced aerobic glycolysis. Aberrant glycolysis in tumoir cells will facilitate the establishment of an immunosuppressive TME, which is vital for cancer cells to escape immune surveillance.[21,52] The fermentation product of glycolysis, mainly lactic acid, has a regulatory role in the T-cell function and further facilitates immune suppression.[22,53,54] Moreover, novel tumor cell targeting drug delivery systems make it possible to target and inhibit tumor glycolysis directly and precisely in experimental setting.[55]

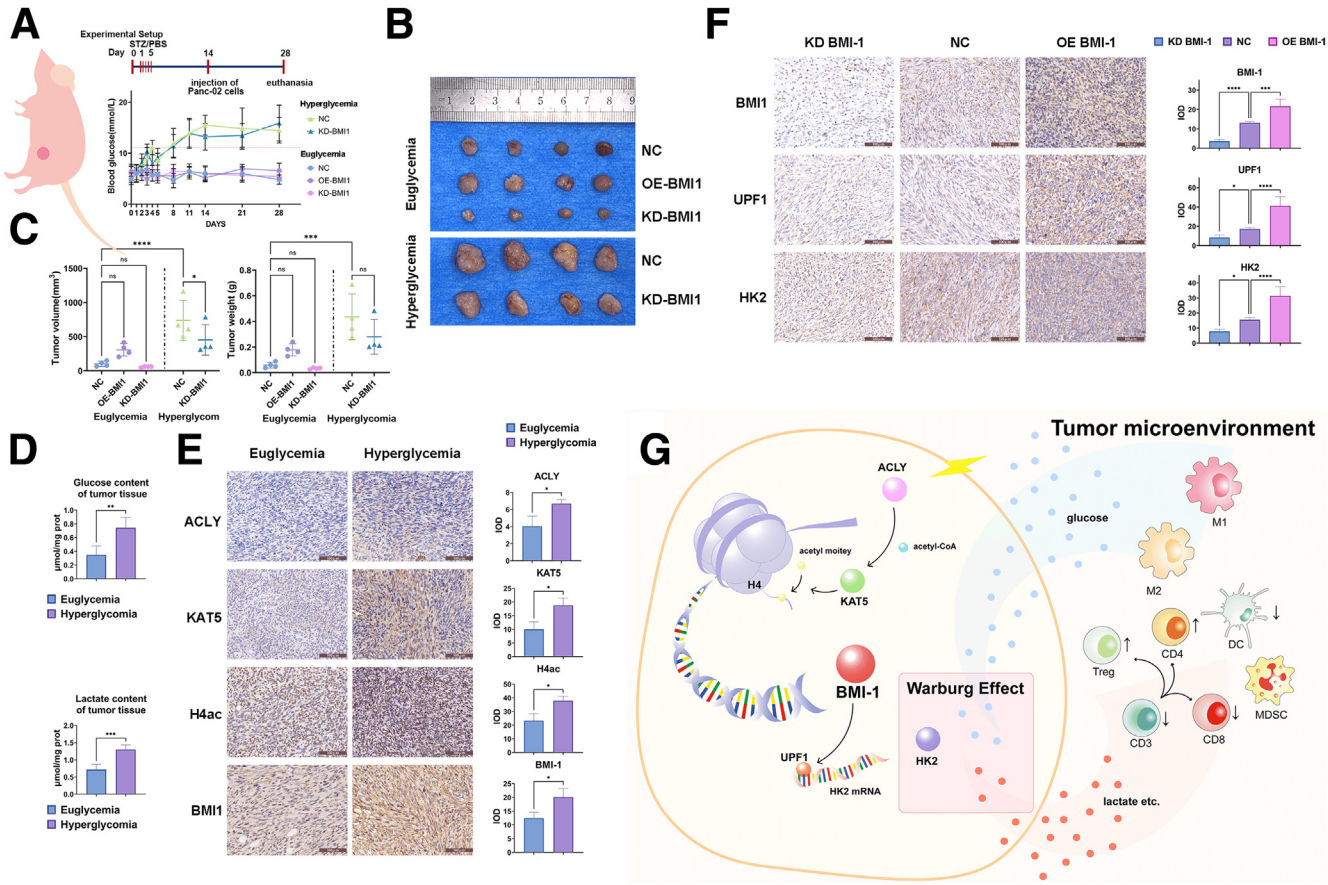

Figure 9. The role of hyperglycemia-induced Bmi1 expression under immunodeficient environment. (*A*) Experimental schema of generating the immunodeficient BALB/c nude mice model; and alterations in blood glucose levels after STZ treatment. (*B*) Representative pictures of the orthotopic tumors. (*C*) Changes in tumor volume and tumor weight in different groups. . (*D*) The lactic acid concentration and glucose concentration of tumor tissues from normal and diabetes animal models. (*E*) IHC staining to evaluate the ACLY, KAT4, H4ac, and Bmi1 protein level in euglycemia-NC and hyperglycemia-NC. (*F*) IHC staining to evaluate Bmi1, UPF1, and HK2 protein level in KD-Bmi1, NC, and OE-Bmi1 in the euglycemia model. (*G*) Schematic diagram showing the effect of the hyperglycemia-Bmi1-HK2 pathway on the Warburg effect and TME. Data presented in the graphs represented means ± standard deviation from 3 parallel experiments. ****$P < .0001$; ***$P < .001$; **$P < .01$; *$P < .05$.

To validate this hypothesis, Bmi1 was silenced in PC cells, which suppressed the effects of high-glucose upregulation of aerobic glycolysis. Our analyses showed that HK2 expression was induced by high-glucose treatment and that Bmi1 silencing blocked the HK2 upregulation. Overexpression of Bmi1 in vivo influenced an assortment of tumor-infiltrating immune cells and established immune-suppressive TME. Importantly, inhibition of HK2 activity by 2-DG or knockdown HK2 expression blocked the high-glucose induction of aerobic glycolysis and Bmi1-induced immune suppression. Under hyperglycemic conditions, knockdown Bmi1 expression in vivo suppressed the anti-tumor immune cell infiltrate, and this effect was also reversed by overexpression of HK2. Evidence from this study supports a relationship among hyperglycemia-induced Bmi1-HK2 pathway activity, Warburg effect enhancement, and cancer cell immunosuppression. In in vitro studies, we have used multiple human PC cells to maximally represent human PC, including SW1990 (with Kras G12D mutation), CFPAC-1 (with Kras G12V mutation), and BxPC-3 (representing wild-type Kras). Our highly consistent results in multiple experiments demonstrate that the correlation and hyperglycemia and aberrant aerobic glycolysis in PC through Bmi1-UPF1-HK2 pathway is not dependent on Kras mutation. Further, recent literature strongly supports the notion that Bmi-1 not only contributes to regulating immunity in pancreatic cancer, but also in other cancer types.[56]

Epigenetic changes adapt environmental alterations, gene expression, and phenotypic state of cells.[57] Cancer cells are particularly sensitive and can adapt to the changes occurred in TME, including fluctuations in energy substrate availability.[58] Cancer cells partially decide to proliferate or undergo apoptosis based on nutrient availability. In addition, metabolites such as acetyl-CoA, S-adenosylmethionine, and flavin adenine dinucleotide are utilized by chromatin-modifying enzymes to affect the transcriptional network that regulates gene expression.[59,60] Acetyl-CoA serves as the

donor for histone acetylation and is reliant on intracellular acetyl-CoA availability,[61-63] which is dynamically regulated by glucose availability in TME.[41] ACLY is a metabolic enzyme found in both cytosol and nucleus that cleaves citrate to generate acetyl-CoA, and plays an essential role in regulating histone acetylation.[41,62] In PC, a high level of histone acetylation is associated with poor survival.[64] Because Bmi1 expression in PC cells was promoted by VPA, a deacetylase inhibitor, whether high glucose promotes Bmi1 expression in PC cells by upregulation of histone acetylation in an ACLY-dependent manner was tested. Our results show that the H4ac level at the promoter region of Bmi1 gene in high glucose-treated cells was significantly higher than that in control cells. In addition, a high glucose TME-enhanced sphere formation ability of PC cells and upregulated the expression of CSC markers including CD133, CD24, Klf4, and Oct4, and pluripotent cell markers including Nanog and Sox2. Taken together, our results suggest that nutrients in pancreatic TME promote cancer stemness via epigenetic modulation, and acetyl-CoA mediates environmental perturbations.

These results demonstrate that Bmi1 regulates the Warburg effect in PC cells and enhances the immunosuppressive TME by targeting HK2. Furthermore, hyperglycemic TME also modulates the epigenetics of PC cells and promotes Bmi1 expression. Epigenetic mechanisms may play a key role in the metabolic alterations and crosstalk between TME and cancer stem-like cell properties. Our research suggests that BMI1 may be a promising target to ameliorate the immunosuppressive microenvironment, and glycemic control is crucial for patients with PC with DM.

Materials and Methods

Cell Lines

Human PC cell lines, SW1990 (with Kras G12D mutation) and BxPC-3 (representing wild-type Kras), were obtained from the American Type Culture Collection (Manassas, VA). Human PC cell line, CFPAC-1 (with Kras G12V mutation), 119 and murine ductal pancreas adenocarcinoma cell line, Panc-02 (representing wild-type Kras with homozygous null mutantion of Smad4), were obtained from Procell (Procell Bio-Tech, Shanghai, China). The cells were tested to confirm the absence of *Mycoplasma* contamination by using the MycoBlue Mycoplasma Detector (Vazyme, Nanjing, China). All cell lines were cultured in Dulbecco's Modified Eagle Medium (DMEM) containing 10% fetal bovine serum (Gibco Invitrogen, Grand Island, NY) and 100 U/mL penicillin/streptomycin (Beyotime Biotechnology, Shanghai, China). General cell culture was performed under normoglycemia condition (5.5 mM D-glucose). To mimic hyperglycemic condition in tissue culture, 2 diabetogenic glucose concentrations (15 mM and 25 mM) were chosen.

Quantitative Real-time Polymerase Chain Reaction Assay

qRT-PCR was performed as previously described.[33,45] The data was interpreted using the $2^{-\Delta\Delta CT}$ method with β-actin as a control. The primer sequences are provided in the Supplementary Materials.

Western Blot Analysis

Western blot was performed as previously described.[34,42] Extraction of proteins was performed with a subcellular structure membrane protein and cytoplasmic protein extraction kit (Boster Biological Technology, China, #AR0155), according to the manufacturer's instructions. Details of the primary antibodies used are provided in the Supplementary Materials.

Determination of Intracellular Acetyl-CoA Levels

Intracellular acetyl-CoA levels in the PC cells were assessed using an acetyl-CoA assay kit from Sigma (#MAK039) following the manufacturer's protocol.

Cell Transfection and Lentivirus Infection

The siRNAs for ACLY , Bmi1, KAT2A, KAT5, and negative control were designed and synthesized by Ribobio (Guangzhou, China). The Bmi1 cDNA overexpression (pcDNA3.1-Bmi1) and empty cDNA vectors (pcDNA3.1-NC) were designed and synthesized by GenePharma (Shanghai, China). Lipofectamine 2000 (Invitrogen, Waltham, MA) was used for cell transfection as per manufacturer's protocol. After transfection for 4 to 6 hours, the medium was replaced with a regular medium. The siRNA sequences are shown in the Supplementary Materials.

NC-short hairpin RNA (shRNA) lentivirus (puromycin resistance), Bmi1-shRNA lentivirus (puromycin resistance), HK2-shRNA lentivirus (blasticidin resistance), Bmi1-overexpression lentivirus (puromycin resistance), and HK2-overexpression lentivirus (blasticidin resistance) were purchased from GeneChem (Shanghai, China). The viral supernatants were used to infect Panc-02 cells. Stable overexpressing-Bmi1(OE-Bmi1), knockdown-Bmi1(KD-Bmi1), OE-Bmi1/knockdown-HK2 (OE-Bmi1/KD-HK2), KD-Bmi1/overexpressing-HK2 (KD-Bmi1/OE-HK2), or KD-HK2 cells were constructed by lentiviral infection. Stable cell lines were selected with 0.5 μg/mL puromycin (OE-Bmi1 cells and KD-Bmi1 cells), 2.5μg/mL blasticidin (KD-HK2 cells), or 0.5 μg/mL puromycin + 2.5 μg/mL blasticidin (OE-Bmi1/KD-HK2 cells and KD-Bmi1/OE-HK2 cells) for 2 days.

Chromatin Immunoprecipitation Assay

ChIP was performed using Simple ChIP Enzymatic Chromatin IP Kit (Agarose Beads) (Cell Signaling Technology, Danvers, MA, #22188), following the manufacturer's protocol. After culturing at 5.5 or 25 mM glucose for 48 hours, ChIP was performed using anti-Histone4ac (Millipore, #17-630) or anti-IgG antibody as a control. The bound DNA fragments were amplified using Bmi1 promoter-specific primers. The primer sequences used in the ChIP-qPCR are shown in the Supplementary Materials.

Lactate Concent, Glucose Concent, and Glucose Uptake Measurements

Lactate and glucose uptake measurements were performed as previously described.[65] Lactate in the supernatant and tumor tissues was determined using the lactic acid assay kit (Nanjing Jiancheng Bio, Nanjing, China, #A019-2-1) as per manufacturer's protocol and correlated with the total protein in each sample. Glucose concent in tumor tissues was determined using the Glucose Content Assay Kit (Solarbio, Beijing, China, # BC2505), as per manufacturer's protocol and correlated with the total protein in each sample. For assessment of glucose uptake, 2-NBDG (2-(*N*-(7-nitrobenz-2-oxa-1,3-diazol-4-yl)Amino)-2-deoxyglucose) (Cayman Chemical, Ann Arbor, MI) uptake was analyzed by flow cytometry.

Flow Cytometry Analysis

Prior to harvest, activated human primary T cells (Stemcell Technologies) were treated for 24 hours and 4 hours, respectively, with a PMA/ionomycin mixture (MultiSciences, Hangzhou, China, #70-CS1001) and brefeldin A (BFA)(Sigma-Aldrich, MO, USA, #B5936). After washing thrice with PBS, the T cells were incubated with CD8 antibody (BD Pharmingen, #555367) at 4 °C in the dark for 30 minutes. The T cells were fixed and permeabilized using the Fixation/Permeabilization Set protocol (eBioscience, CA, #00-5123-43, #00-5223-56, #00-8333-56) and incubated with IFNγ antibody (BD Pharmingen, #554700) in the dark for 30 minutes. After washing twice, the T cells were analyzed through flow cytometry.

Single-cell suspensions of tumor-infiltrated immune cells from animal experiments were prepared. To minimize nonspecific binding, cells were then incubated with anti-CD16/CD32 antibody (BD Pharmingen, #553141). All cell surface reactions (CD45, CD3, CD4, CD8, CD25, I-A/I-E, CD11c, CD11b, F4/80, PD-1, CD86, Ly-6G, and Ly-6C) were performed at 4 °C for 30 minutes. The permeabilization step allowing intracellular staining (KI-67, IFN-γ, GZMB, Perforin, and Foxp3) was performed according to the manufacturer's recommendations (BD Pharmingen, # 562574, #550583). After being washed thrice, the sample cells were suspended in PBS at a concentration of 10^6/200 μL and analyzed by flow cytometry. The fluorochrome-conjugated antimouse antibodies used in the present study are listed in the Supplementary Materials, and the gating strategy is shown in Figure 10.

Sphere-forming Assay

PC cells were grown in serum-free DMEM/F12 media supplemented with 2% B-27 (Gibco, #17504044), heparin (4 μg/mL), epidermal growth factor (20 ng/mL) (R&D, #236-EG-200), and fibroblast growth factor (20 ng/mL) (PEPROTECH, #AF-100-18C). DMEM/F12 media with different glucose concentrations were made by mixing equal volumes of DMEM low-glucose media (Gibco) and F12 media (Gibco) supplemented with D-glucose (Aladdin Industrial Corporation, Shanghai, China, #G116304). The assay was performed using 500 cells per well on ultra-low attachment 6-well plates. After 7 days, the cultures were analyzed under a phase-contrast light microscope for sphere formation.

RNA Immunoprecipitation Assay

RNA immunoprecipitation was performed using an anti-UPF1 antibody (Proteintech, Wuhan, China, #23379-1-AP) and the RBP Immunoprecipitation Kit (Sigma-Aldrich, St Louis, MO, #17-700) following the manufacturer's protocol.

Murine Models

All experiments involving animals in this research followed the ethical standards set by the Institutional Animal Care and Use Committee of Tongji Medical College, Huazhong University of Science and Technology. Five-week-old male C57BL/6 mice and 5-week-old BALB/c Nude mice were purchased from China Three Gorges University. C57BL/6 mice and BALB/c Nude mice were divided randomly into control and diabetes groups. For the diabetes group, mice were injected for 5 consecutive days with 50 mg/kg STZ (Sigma, St. Louis, MO, #S0130) dissolved in cold fresh sodium citrate buffer (pH = 4.5). Sannuo glucometer (Sannuo, Changsha, China) was used to measure the glucose levels in blood samples taken from tail vein. Mice with blood glucose levels $\geq$11.1 mmol/L were selected as the diabetic mice.

Subcutaneous Panc-02 Model in Immune-competent C57BL/6 Mice

For evaluating the effects of hyperglycemia and hyperglycemia-induced aerobic glycolysis in immune suppression. Subcutaneous Panc-02 tumors (n = 5 in each group) were generated in immune-competent C57BL/6 mice. Tumors were created by injecting 10^6 cells in 100 μL PBS under the skin of the left flank in both control and diabetes groups. Seven days after injection, 2-DG (5 mM, 50 μL, Sigma-Aldrich, #D8375) or PBS (50 μL) were locally injected around the tumor mass at multiple points every 2 days for 6 times total. Three weeks after injection of the stable Panc-02 cells, the mice were sacrificed.

Orthotopic Panc-02 Model in Immune-competent C57BL/6 Mice

To evaluate the function of Bmi1-HK2 in hyperglycemia-induced immune suppression, Panc-02 cells transfected with NC, OE-Bmi1, KD-Bmi1, OE-Bmi1/KD-HK2, KD-Bmi1/OE-HK2, or KD-HK2 lentivirus were injected into the C57BL/6 mouse pancreas tail in both control and diabetes groups by laparotomy. Briefly, mice (n = 4 in each group) were anesthetized with an intraperitoneal injection of 1.25% tribromoethanol (20 μL/g mouse). Fur was shaved in the left-flank surgical field using an electric clipper, and the region of the incision was sterilized with betadine. PC cells were injected (1×10^6 cells) in 10 μL PBS + 10 μL Matrigel in the tail of pancreas that was exposed under the left-flank incision. Three weeks after injection of the stable Panc-02 cells, the mice were sacrificed.

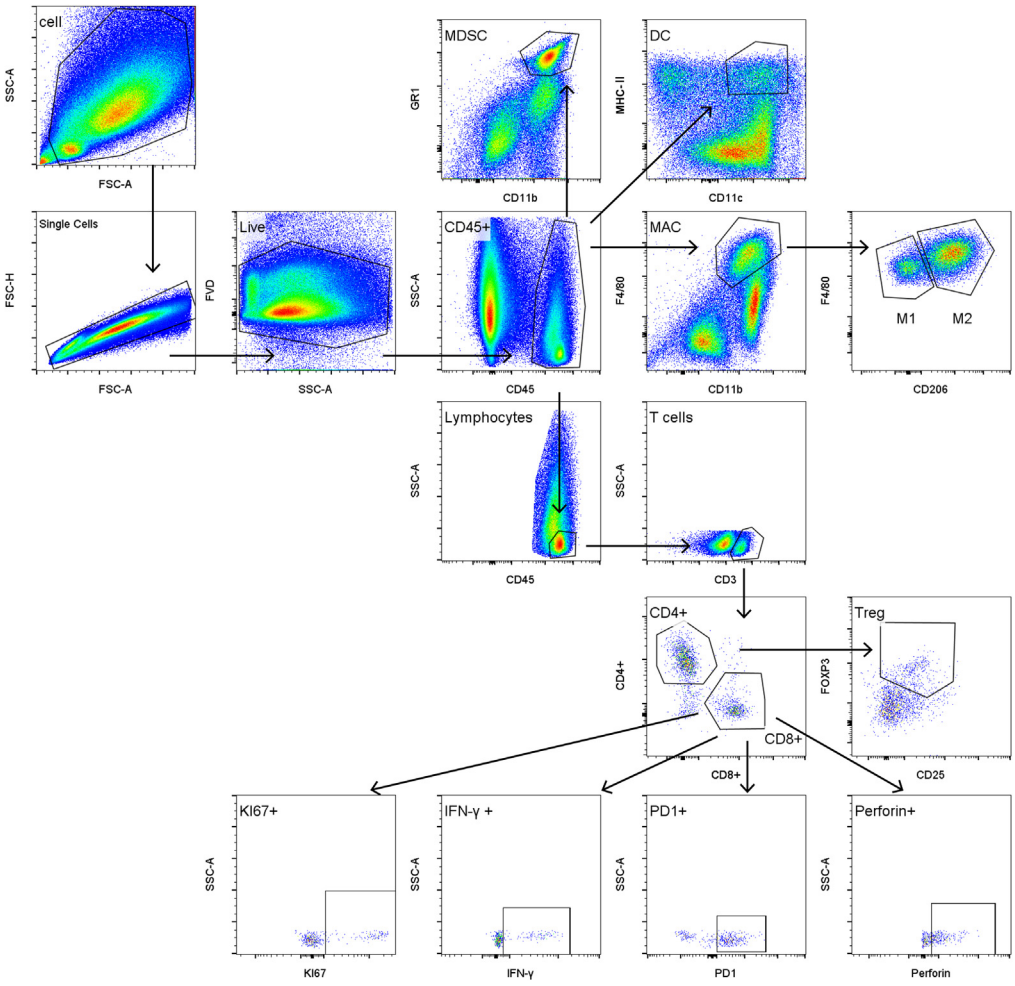

Figure 10. Flowcytometry gating strategy.

Subcutaneous Panc-02 Model in Immunodeficient BALB/c Nude Mice

To evaluate the role of Bmi1 in tumorigenesis under an immunodeficient environment, Panc-02 cells transfected with NC, OE-Bmi1, KD-Bmi1 lentivirus were injected subcutaneously (1×10^6 cells/100 μL/mouse) into the left flank of BALB/c nude mice in both control and diabetes groups. Two weeks after injection of the stable Panc-02 cells, the mice were sacrificed.

Immunohistochemistry

IHC was performed as previously described.[65] Antibody information is available in the Supplemental Materials. The average immunity group image gradation analysis integral light density of Bmi1, UPF1, HK2, ACLY, KAT5, and H4ac in 5 randomly selected areas for each group were calculated by using Imagepro Plus 6.0 (Media Cybernetics, Inc).

mRNA Half-life Assay

PC cells transfected with ncRNA or UPF1 siRNA were treated with 5 μg/mL actinomycin D (Sellect, USA, #S8964). PC cells were then collected at 0, 1, 2, 4, 8, and 16 hours after the supplementation of actinomycin D, and qPCR was performed to measure the levels of HK2 mRNA.

Statistical Analysis

Statistical power was calculated with GraphPad Prism 9.3.1. The results are shown as the mean ± standard deviation. Comparisons between 2 groups or multiple groups were analyzed using the Student *t* test or 1-way analysis of variance. All tests were 2-sided; a *P*-value $< .05$ was considered statistically significant.

Gene Expression Datasets

The transcriptome data of 2 independent cohorts (E-MTAB-6134 and E-MTAB-1791) used in this study was obtained from public domain (ArrayExpress, https://www.ebi.ac.uk/arrayexpress).

Activity Detection of Molecular Metabolic Pathways

Gene Set Variation Analysis used the Gene Set Variation Analysis package of R-3.6.1.[66,67] Enrichment score was considered to be the measure of metabolic intensity for

subsequent analyses and calculations (Supplementary Table 1 and c2.all.v7.1.symbols from Molecular Signatures Database v7.2).

Inferred Abundances of Immune Subsets

Xcell (http://xCell.ucsf.edu/) was used to infer 64 immune and stromal cell types based on single-sample Gene Set Enrichment Analysis.[68] The default parameter P-value $<$ .2 was used as the criterion of reliability.

Survival Analysis

Overall survival time was used as the single criterion for survival analysis. Survival curves were drawn using the survival package of R.

Correlation Analyses

Correlations between continuous variables were tested using the Hmisc package (version 4.2-0) of R, based on the Spearman correlation coefficient.

Variation Analysis

Variation in infiltrating immune cell proportions between samples with high- or low-level intensity of glycolysis was determined using the Kruskal-Wallis test.

References

1. Ko AH, Tempero MA. Personalized medicine for pancreatic cancer: a step in the right direction. Gastroenterology 2009;136:43–45.
2. Wolfgang CL, Herman JM, Laheru DA, Klein AP, Erdek MA, Fishman EK, Hruban RH. Recent progress in pancreatic cancer. CA Cancer J Clin 2013;63:318–348.
3. Maisonneuve P, Lowenfels AB. Risk factors for pancreatic cancer: a summary review of meta-analytical studies. Int J Epidemiol 2015;44:186–198.
4. Andersen DK, Andren-Sandberg A, Duell EJ, Goggins M, Korc M, Petersen GM, Smith JP, Whitcomb DC. Pancreatitis-diabetes-pancreatic cancer: summary of an NIDDK-NCI workshop. Pancreas 2013;42:1227–1237.
5. Hidalgo M. Pancreatic cancer. N Engl J Med 2010; 362:1605–1617.
6. Huxley R, Ansary-Moghaddam A, Berrington de Gonzalez A, Barzi F, Woodward M. Type-II diabetes and pancreatic cancer: a meta-analysis of 36 studies. Br J Cancer 2005;92:2076–2083.
7. Ben Q, Xu M, Ning X, Liu J, Hong S, Huang W, Zhang H, Li Z. Diabetes mellitus and risk of pancreatic cancer: a meta-analysis of cohort studies. Eur J Cancer 2011; 47:1928–1937.
8. Raghavan SR, Ballehaninna UK, Chamberlain RS. The impact of perioperative blood glucose levels on pancreatic cancer prognosis and surgical outcomes: an evidence-based review. Pancreas 2013;42:1210–1217.
9. Yuan C, Rubinson DA, Qian ZR, Wu C, Kraft P, Bao Y, Ogino S, Ng K, Clancy TE, Swanson RS. Survival among patients with pancreatic cancer and long-standing or recent-onset diabetes mellitus. J Clin Oncol 2015; 33:29–35.
10. Toriola AT, Stolzenberg-Solomon R, Dalidowitz L, Linehan D, Colditz G. Diabetes and pancreatic cancer survival: a prospective cohort-based study. Br J Cancer 2014;111:181–185.
11. Kleeff J, Costello E, Jackson R, Halloran C, Greenhalf W, Ghaneh P, Lamb RF, Lerch MM, Mayerle J, Palmer D, Cox T, Rawcliffe CL, Strobel O, Buchler MW. The impact of diabetes mellitus on survival following resection and adjuvant chemotherapy for pancreatic cancer. Br J Cancer 2016;115:887–894.
12. Giovannucci E, Michaud D. The role of obesity and related metabolic disturbances in cancers of the colon, prostate, and pancreas. Gastroenterology 2007; 132:2208–2225.
13. Krone CA, Ely JTA. Controlling hyperglycemia as an adjunct to cancer therapy. Integr Cancer Ther 2005; 4:25–31.
14. Warburg O. On the origin of cancer cells. Science 1956; 123:309–314.
15. Han J, Zhang L, Guo H, Wysham WZ, Roque DR, Willson AK, Sheng X, Zhou C, Bae-Jump VL. Glucose promotes cell proliferation, glucose uptake and invasion in endometrial cancer cells via AMPK/mTOR/S6 and MAPK signaling. Gynecol Oncol 2015;138:668–675.
16. Liu Z, Jia X, Duan Y, Xiao H, Sundqvist K-G, Permert J, Wang F. Excess glucose induces hypoxia-inducible factor-1α in pancreatic cancer cells and stimulates glucose metabolism and cell migration. Cancer Biol Ther 2013;14:428–435.
17. Qiu J, Villa M, Sanin DE, Buck MD, O'Sullivan D, Ching R, Matsushita M, Grzes KM, Winkler F, Chang CH, Curtis JD, Kyle RL, Van Teijlingen Bakker N, Corrado M, Haessler F, Alfei F, Edwards-Hicks J, Maggi LB Jr, Zehn D, Egawa T, Bengsch B, Klein Geltink RI, Jenuwein T, Pearce EJ, Pearce EL. Acetate promotes T cell effector function during glucose restriction. Cell Rep 2019;27:2063–2074.e5.
18. Sukumar M, Roychoudhuri R, Restifo NP. Nutrient competition: a new axis of tumor immunosuppression. Cell 2015;162:1206–1208.
19. Harmon C, O'Farrelly C, Robinson MW. The immune consequences of lactate in the tumor microenvironment. Adv Exp Med Biol 2020;1259:113–124.
20. Huber V, Camisaschi C, Berzi A, Ferro S, Lugini L, Triulzi T, Tuccitto A, Tagliabue E, Castelli C, Rivoltini L. Cancer acidity: an ultimate frontier of tumor immune escape and a novel target of immunomodulation. Semin Cancer Biol 2017;43:74–89.
21. Lim SO, Li CW, Xia W, Lee HH, Chang SS, Shen J, Hsu JL, Raftery D, Djukovic D, Gu H, Chang WC, Wang HL, Chen ML, Huo L, Chen CH, Wu Y, Sahin A, Hanash SM, Hortobagyi GN, Hung MC. EGFR signaling enhances aerobic glycolysis in triple-negative breast cancer cells to promote tumor growth and immune escape. Cancer Res 2016;76:1284–1296.
22. Fischer K, Hoffmann P, Voelkl S, Meidenbauer N, Ammer J, Edinger M, Gottfried E, Schwarz S, Rothe G, Hoves S, Renner K, Timischl B, Mackensen A, Kunz-

Schughart L, Andreesen R, Krause SW, Kreutz M. Inhibitory effect of tumor cell-derived lactic acid on human T cells. Blood 2007;109:3812–3819.
23. Chang C-H, Qiu J, O'Sullivan D, Buck MD, Noguchi T, Curtis JD, Chen Q, Gindin M, Gubin MM, Van Der Windt GJW, Tonc E, Schreiber RD, Pearce EJ, Pearce EL. Metabolic competition in the tumor microenvironment is a driver of cancer progression. Cell 2015; 162:1229–1241.
24. Kareva I, Hahnfeldt P. The emerging "hallmarks" of metabolic reprogramming and immune evasion: distinct or linked? Cancer Res 2013;73:2737–2742.
25. Chowdhury M, Mihara K, Yasunaga S, Ohtaki M, Takihara Y, Kimura A. Expression of Polycomb-group (PcG) protein BMI-1 predicts prognosis in patients with acute myeloid leukemia. Leukemia 2007;21:1116–1122.
26. Xiao JF, Sun QY, Ding LW, Chien W, Liu XY, Mayakonda A, Jiang YY, Loh XY, Ran XB, Doan NB, Castor B, Chia D, Said JW, Tan KT, Yang H, Fu XY, Lin DC, Koeffler HP. The c-MYC–BMI1 axis is essential for SETDB1-mediated breast tumourigenesis. J Pathol 2018;246:89–102.
27. Wang HB, Liu GH, Zhang H, Xing S, Hu LJ, Zhao WF, Xie B, Li MZ, Zeng BH, Li Y, Zeng MS. Sp1 and c-Myc regulate transcription of BMI1 in nasopharyngeal carcinoma. FEBS J 2013;280:2929–2944.
28. Song W, Tao K, Li H, Jin C, Song Z, Li J, Shi H, Li X, Dang Z, Dou K. Bmi-1 is related to proliferation, survival and poor prognosis in pancreatic cancer. Cancer Sci 2010;101:1754–1760.
29. Bednar F, Schofield HK, Collins MA, Yan W, Zhang Y, Shyam N, Eberle JA, Almada LL, Olive KP, Bardeesy N, Fernandez-Zapico ME, Nakada D, Simeone DM, Morrison SJ, Pascia di Magliano M. Bmi1 is required for the initiation of pancreatic cancer through an Ink4a-independent mechanism. Carcinogenesis 2015;36:730–738.
30. Mustafi SB, Chakraborty PK, Naz S, Dwivedi SKD, Street M, Basak R, Yang D, Ding K, Mukherjee P, Bhattacharya R. MDR1 mediated chemoresistance: BMI1 and TIP60 in action. Biochim Biophys Acta 2016; 1859:983–993.
31. He Q, Liu Z, Zhao T, Zhao L, Zhou X, Wang A. Bmi1 drives stem-like properties and is associated with migration, invasion, and poor prognosis in tongue squamous cell carcinoma. Int J Biol Sci 2015;11:1–10.
32. Park I-k, Qian D, Kiel M, Becker MW, Pihalja M, Weissman IL, Morrison SJ, Clarke MF. Bmi-1 is required for maintenance of adult self-renewing haematopoietic stem cells. Nature 2003;423:302–305.
33. Valk-Lingbeek ME, Bruggeman SW, van Lohuizen M. Stem cells and cancer; the polycomb connection. Cell 2004;118:409–418.
34. Duan Q, Li H, Gao C, Zhao H, Wu S, Wu H, Wang C, Shen Q, Yin T. High glucose promotes pancreatic cancer cells to escape from immune surveillance via AMPK-Bmi1-GATA2-MICA/B pathway. J Exp Clin Cancer Res 2019;38:192.
35. Sparmann A, van Lohuizen M. Polycomb silencers control cell fate, development and cancer. Nat Rev Cancer 2006;6:846–856.
36. Rhodes DR, Yu J, Shanker K, Deshpande N, Varambally R, Ghosh D, Barrette T, Pandey A, Chinnaiyan AM. ONCOMINE: a cancer microarray database and integrated data-mining platform. Neoplasia 2004;6:1–6.
37. Badea L, Herlea V, Dima SO, Dumitrascu T, Popescu I. Combined gene expression analysis of whole-tissue and microdissected pancreatic ductal adenocarcinoma identifies genes specifically overexpressed in tumor epithelia. Hepatogastroenterology 2008;55:2016–2027.
38. Hanahan D, Weinberg RA. Hallmarks of cancer: the next generation. Cell 2011;144:646–674.
39. Perusina Lanfranca M, Thompson JK, Bednar F, Halbrook C, Lyssiotis C, Levi B, Frankel TL. Metabolism and epigenetics of pancreatic cancer stem cells. Semin Cancer Biol 2019;57:19–26.
40. Flavahan WA, Wu Q, Hitomi M, Rahim N, Kim Y, Sloan AE, Weil RJ, Nakano I, Sarkaria JN, Stringer BW, Day BW, Li M, Lathia JD, Rich JN, Hjelmeland AB. Brain tumor initiating cells adapt to restricted nutrition through preferential glucose uptake. Nat Neurosci 2013;16:1373–1382.
41. Lee JV, Carrer A, Shah S, Snyder NW, Wei S, Venneti S, Worth AJ, Yuan ZF, Lim HW, Liu S, Jackson E, Aiello NM, Haas NB, Rebbeck TR, Judkins A, Won KJ, Chodosh LA, Garcia BA, Stanger BZ, Feldman MD, Blair IA, Wellen KE. Akt-dependent metabolic reprogramming regulates tumor cell histone acetylation. Cell Metab 2014; 20:306–319.
42. Li H, Zhang Z, Gao C, Wu S, Duan Q, Wu H, Wang C, Shen Q, Yin T. Combination chemotherapy of valproic acid (VPA) and gemcitabine regulates STAT3/Bmi1 pathway to differentially potentiate the motility of pancreatic cancer cells. Cell Biosci 2019;9:50.
43. Li D. Diabetes and pancreatic cancer. Mol Carcinog 2012;51:64–74.
44. Cui Y, Andersen DK. Diabetes and pancreatic cancer. Endocr Relat Cancer 2012;19:F9–F26.
45. Pannala R, Leirness JB, Bamlet WR, Basu A, Petersen GM, Chari ST. Prevalence and clinical profile of pancreatic cancer-associated diabetes mellitus. Gastroenterology 2008;134:981–987.
46. Pelaez-Luna M, Takahashi N, Fletcher JG, Chari ST. Resectability of presymptomatic pancreatic cancer and its relationship to onset of diabetes: a retrospective review of CT scans and fasting glucose values prior to diagnosis. Am J Gastroenterol 2007;102:2157–2163.
47. Andersen DK, Korc M, Petersen GM, Eibl G, Li D, Rickels MR, Chari ST, Abbruzzese JL. Diabetes, pancreatogenic diabetes, and pancreatic cancer. Diabetes 2017;66:1103–1110.
48. Li W, Zhang L, Chen X, Jiang Z, Zong L, Ma Q. Hyperglycemia promotes the epithelial-mesenchymal transition of pancreatic cancer via hydrogen peroxide. Oxid Med Cell Longev 2016;2016:5190314.
49. Han L, Ma Q, Li J, Liu H, Li W, Ma G, Xu Q, Zhou S, Wu E. High glucose promotes pancreatic cancer cell proliferation via the induction of EGF expression and transactivation of EGFR. PLoS One 2011;6:e27074.
50. Vander Heiden MG, Cantley LC, Thompson CB. Understanding the Warburg effect: the metabolic requirements of cell proliferation. Science 2009;324:1029–1033.

51. Liberti MV, Locasale JW. The Warburg effect: how does it benefit cancer cells? Trends Biochem Sci 2016; 41:211–218.
52. Cascone T, McKenzie JA, Mbofung RM, Punt S, Wang Z, Xu C, Williams LJ, Wang Z, Bristow CA, Carugo A, Peoples MD, Li L, Karpinets T, Huang L, Malu S, Creasy C, Leahey SE, Chen J, Chen Y, Pelicano H, Bernatchez C, Gopal YNV, Heffernan TP, Hu J, Wang J, Amaria RN, Garraway LA, Huang P, Yang P, Wistuba II, Woodman SE, Roszik J, Davis RE, Davies MA, Heymach JV, Hwu P, Peng W. Increased tumor glycolysis characterizes immune resistance to adoptive T cell therapy. Cell Metab 2018;27:977–987.e4.
53. Doherty JR, Cleveland JL. Targeting lactate metabolism for cancer therapeutics. J Clin Invest 2013;123:3685–3692.
54. Brand A, Singer K, Koehl GE, Kolitzus M, Schoenhammer G, Thiel A, Matos C, Bruss C, Klobuch S, Peter K, Kastenberger M, Bogdan C, Schleicher U, Mackensen A, Ullrich E, Fichtner-Feigl S, Kesselring R, Mack M, Ritter U, Schmid M, Blank C, Dettmer K, Oefner PJ, Hoffmann P, Walenta S, Geissler EK, Pouyssegur J, Villunger A, Steven A, Seliger B, Schreml S, Haferkamp S, Kohl E, Karrer S, Berneburg M, Herr W, Mueller-Klieser W, Renner K, Kreutz M. LDHA-associated lactic acid production blunts tumor immunosurveillance by T and NK cells. Cell Metab 2016;24:657–671.
55. Sasaki K, Nishina S, Yamauchi A, Fukuda K, Hara Y, Yamamura M, Egashira K, Hino K. Nanoparticle-mediated delivery of 2-Deoxy-D-glucose induces antitumor immunity and cytotoxicity in liver tumors in mice. Cell Mol Gastroenterol Hepatol 2021;11:739–762.
56. Jia L, Zhang W, Wang CY. BMI1 Inhibition eliminates residual cancer stem cells after PD1 blockade and activates antitumor immunity to prevent metastasis and relapse. Cell Stem Cell 2020;27:238–253.e6.
57. Wainwright EN, Scaffidi P. Epigenetics and cancer stem cells: unleashing, hijacking, and restricting cellular plasticity. Trends Cancer 2017;3:372–386.
58. Gut P, Verdin E. The nexus of chromatin regulation and intermediary metabolism. Nature 2013;502:489–498.
59. Shi Y, Shi Y. Metabolic enzymes and coenzymes in transcription–a direct link between metabolism and transcription? Trends Genet 2004;20:445–452.
60. Ladurner AG. Rheostat control of gene expression by metabolites. Mol Cell 2006;24:1–11.
61. Wellen KE, Hatzivassiliou G, Sachdeva UM, Bui TV, Cross JR, Thompson CB. ATP-citrate lyase links cellular metabolism to histone acetylation. Science 2009; 324:1076–1080.
62. Carrer A, Wellen KE. Metabolism and epigenetics: a link cancer cells exploit. Curr Opin Biotechnol 2015;34:23–29.
63. Shi L, Tu BP. Acetyl-CoA and the regulation of metabolism: mechanisms and consequences. Curr Opin Cell Biol 2015;33:125–131.
64. Juliano CN, Izetti P, Pereira MP, Dos Santos AP, Bravosi CP, Abujamra AL, Prolla PA, Osvaldt AB, Edelweiss MI. H4K12 and H3K18 acetylation associates with poor prognosis in pancreatic cancer. Appl Immunohistochem Mol Morphol 2016;24:337–344.
65. Zhao H, Wu S, Li H, Duan Q, Zhang Z, Shen Q, Wang C, Yin T. ROS/KRAS/AMPK signaling contributes to gemcitabine-induced stem-like cell properties in pancreatic cancer. Mol Ther Oncolytics 2019;14:299–312.
66. Hanzelmann S, Castelo R, Guinney J. GSVA: gene set variation analysis for microarray and RNA-seq data. BMC Bioinformatics 2013;14:7.
67. Yang CS, Stampouloglou E, Kingston NM, Zhang L, Monti S, Varelas X. Glutamine-utilizing transaminases are a metabolic vulnerability of TAZ/YAP-activated cancer cells. EMBO Rep 2018;19:e43577.
68. Aran D, Hu Z, Butte AJ. xCell: digitally portraying the tissue cellular heterogeneity landscape. Genome Biol 2017;18:220.

Received March 9, 2022. Accepted July 11, 2022.

Correspondence
Address correspondence to: Tao Yin, MD, PhD, Department of Pancreatic Surgery, Union Hospital, Tongji Medical College, Huazhong University of Science and Technology, Wuhan 430022, China. e-mail: ytwhun@hust.edu.cn; Tel: +86 027-85351631.

Acknowledgment
The authors thank the Huazhong University of Science & Technology Analytical & Testing center, Medical sub-center for the technical support. The authors thank Dr Long Yu and Mr Libo Luo for their help in flow cytometry technical support.

CRediT Authorship Contributions

Wu Shihong, MD (Conceptualization: Lead; Data curation: Lead; Formal analysis: Lead; Methodology: Lead; Resources: Lead; Visualization: Lead; Writing – original draft: Lead; Writing – review & editing: Lead)

Haoxiang Zhang, MD (Conceptualization: Lead; Data curation: Lead; Formal analysis: Lead; Methodology: Lead; Resources: Lead; Software: Lead; Visualization: Lead; Writing – original draft: Lead; Writing – review & editing: Lead)

Chenggang Gao, MD (Conceptualization: Lead; Data curation: Lead; Formal analysis: Lead; Methodology: Lead; Resources: Lead; Software: Lead; Visualization: Lead; Writing – original draft: Lead)

Jiaoshun Chen, MD (Data curation: Equal; Methodology: Equal; Resources: Equal; Visualization: Equal; Writing – original draft: Equal; Writing – review & editing: Equal)

Hehe Li, MD (Conceptualization: Equal; Data curation: Equal; Methodology: Equal; Resources: Equal; Writing – review & editing: Equal)

Zibo Meng, MD (Methodology: Equal; Resources: Equal; Visualization: Equal; Writing – review & editing: Equal)

Jianwei Bai, MD (Methodology: Equal; Resources: Equal; Visualization: Equal; Writing – review & editing: Equal)

Heshui Wu, MD, PhD (Supervision: Equal; Validation: Equal; Writing – review & editing: Equal)

Qiang Shen, MD, PhD (Visualization: Equal; Writing – review & editing: Lead)

Yin Tao, MD, PhD (Conceptualization: Lead; Data curation: Lead; Formal analysis: Lead; Funding acquisition: Lead; Methodology: Lead; Project administration: Lead; Resources: Lead; Supervision: Lead; Validation: Lead; Visualization: Lead; Writing – original draft: Lead; Writing – review & editing: Lead)

Conflicts of interest
The authors disclose no conflicts.

Funding
This work was supported by the National Natural Science Foundation of China (81772564 , 82173196).